ELSEVIER

Engineering Analysis with Boundary Elements 28 (2004) 79–96

ENGINEERING ANALYSIS *with* BOUNDARY ELEMENTS

www.elsevier.com/locate/enganabound

The collocation Trefftz method for biharmonic equations with crack singularities

Zi-Cai Li*, Tzon-Tzer Lu, Hsin-Yun Hu

Department of Applied Mathematics, National Sun Yat-sen University, Kaohsiung 80424, Taiwan, ROC

Abstract

The purpose of this paper is to extend the boundary approximation method proposed by Li et al. [SIAM J. Numer. Anal. 24 (1987) 487], i.e. the collocation Trefftz method called in this paper, for biharmonic equations with singularities. First, this paper derives the Green formulas for biharmonic equations on bounded domains with a non-smooth boundary, and corner terms are developed. The Green formulas are important to provide all the exterior and interior boundary conditions which will be used in the collocation Trefftz method. Second, this paper proposes three crack models (called Models I, II and III), and the collocation Trefftz method provides their most accurate solutions. In fact, Models I and II resemble Motz's problem in Li et al. [SIAM J. Numer. Anal. 24 (1987) 487], and Model III with all the clamped boundary conditions originated from Schiff et al. [The mathematics of finite elements and applications III, 1979]. Moreover, effects on d_1 of different boundary conditions are investigated, and a brief analysis of error bounds for the collocation Trefftz method is made. Since accuracy of the solutions obtained in this paper is very high, they can be used as the typical models in testing numerical methods. The computed results show that as the singularity models, Models I and II are superior to Model III, because more accurate solutions can be obtained by the collocation Trefftz method.

Keywords: Biharmonic equation; Boundary condition; Corner condition; Green function; Singular problems; Collocation Trefftz methods; Boundary approximation method

1. Introduction

When an interior crack occurs within a thin elastic plate, determination of a stress intensity factor at the crack front is significant in fracture mechanics. Such a mechanical problem can be described as the biharmonic equations with the crack singularity, and the stress intensity factor is given by $K = \sqrt{2\pi}d_1$, where d_1 is the leading coefficient of singular particular solutions.

The singular problems have drawn much attention in the last several decades, and reported in many papers. Most of them deal with the second order partial differential equations (PDEs) including the singular boundary layers [28]. There exist a few books and papers for the fourth order PDEs, such as the biharmonic equations with crack singularities, see Grisvard [8], Lefeber [18], Schiff et al. [30], Whiteman [33], Russo [29], and Karageorghis [15]. Some textbooks and papers for biharmonic equations by the finite element method, the finite difference method, and the boundary element method are given by Chien [5], Oden and Carey [4], Birkhoff and Lynch [2], Arad et al. [1] and Brebbia and Dominguez [3]. In this paper, we pursue better crack models with series expansion solutions of very high convergent rates. Three crack models are found: Models I and II mimic Motz's problem in Ref. [26], and Model III results from Schiff et al. [30]. The Trefftz method was proposed in Ref. [32] in 1926, and several researches have been studied in mathematical aspects and applications of Trefftz methods, e.g. Jin, Cheung and Zienkiewicz [13], Herrera [11], Jirousek and Guex [14], Kita and Kamiya [16] and Piltner and Taylor [27]. The use of the term, Trefftz means boundary collocation, is somewhat recent but several authors used collocation Trefftz approaches such as Kolodziej [17], Herrera and Diaz [10], and Leitao [19] for singular problems. In parallel, the boundary approximation method (BAM) was studied by Li et al. in Refs. [20–23], which is, indeed, the collocation Trefftz method called in this paper. It is noted that Li et al. [20] provide the most accurate solutions for Motz's problem in double precision, with the 35 leading expansion coefficients, although a typo-error of one coefficient was pointed out by Lucas and Oh

* Corresponding author. Tel.: +886-7-5252-000; fax: +886-7-5253-824.
E-mail address: zcli@math.nsysu.edu.tw (Z.-C. Li).

0955-7997/04/$ - see front matter © 2003 Elsevier Ltd. All rights reserved.
doi:10.1016/S0955-7997(03)00094-8

in Ref. [24]. More detailed discussions about the model of Schiff et al. are provided by Hsu [12]. Also the collocation Trefftz method was applied to the interface problems and the unbounded domain problems in Refs. [21,22]. In this paper, the collocation Trefftz method is developed to compute very accurate solutions for the crack models of biharmonic equations.

This paper is organized as follows. In Section 2, we derive the Green formulas for rectangular and polygonal domains, and provide different types of boundary conditions. In Section 3, three crack models are developed, and the collocation Trefftz method is described. In Sections 4 and 5, a brief analysis for the collocation Trefftz method is made, and the collocation Trefftz method is applied to the interior boundary. In Section 6, numerical experiments are carried out to provide very accurate solutions for three models, and in Section 7 concluding remarks are addressed.

2. The Green formulas of $\Delta^2 u$

2.1. On rectangular domains

First, consider the rectangular domain $S = \{(x, y), 0 < x < a, 0 < y < b\}$. We will derive the following Green formulas for $\Delta^2 u$,

$$\int\int_S \Lambda_\mu(u, v) = \int\int_S v\Delta^2 u - \int_{\partial S} m(u)v_n - \int_{\partial S} p(u)v + 2(1-\mu)([u_{xy}v]_3^4 - [u_{xy}v]_1^2), \tag{2.1}$$

where $\Delta u = (\partial^2 u/\partial x^2) + (\partial^2 u/\partial y^2)$, $[v]_1^2 = v_2 - v_1$, and 1, 2, 3, 4 are four corners of S, see Fig. 1. The notations are

$$\begin{aligned}\Lambda_\mu(u, v) &= \Delta u\,\Delta v + (1-\mu)(2u_{xy}v_{xy} - u_{xx}v_{yy} - u_{yy}v_{xx}) \\ &= u_{xx}v_{xx} + u_{yy}v_{yy} + \mu(u_{xx}v_{yy} + u_{yy}v_{xx}) \\ &\quad + 2(1-\mu)u_{xy}v_{xy},\end{aligned} \tag{2.2}$$

$$m(u) = -u_{nn} - \mu u_{ss}, \quad p(u) = u_{nnn} + (2-\mu)u_{ssn}, \tag{2.3}$$

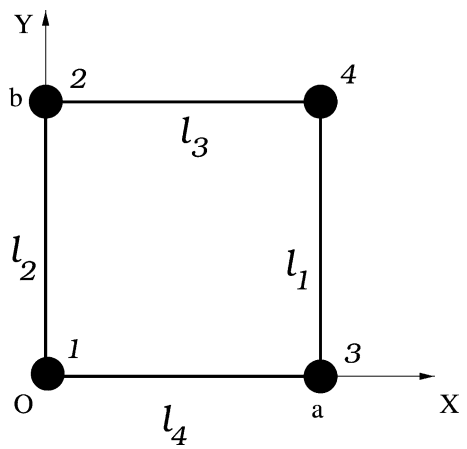

Fig. 1. A rectangle.

where $0 \le \mu < 1$ and n and s are normal and tangent directions along the boundary ∂S of S, respectively, and $u_{xy} = \partial^2 u/\partial x\,\partial y$, $u_{xx} = \partial^2 u/\partial x^2$, $u_{nn} = \partial^2 u/\partial n^2$, $u_{ss} = \partial^2 u/\partial s^2$, etc. In Eq. (2.1), we assume that all integrands wherein are continuous.

In Fig. 1, let ℓ_i with $i = 1, 2, 3, 4$ denote four edges of S, we obtain from integration by parts,

$$\begin{aligned}\int\int_S u_{xx}v_{xx} &= \left(\int_{\ell_1} - \int_{\ell_2}\right) v_x u_{xx} - \int\int_S v_x u_{xxx} \\ &= \left(\int_{\ell_1} - \int_{\ell_2}\right) v_x u_{xx} - \left(\int_{\ell_1} - \int_{\ell_2}\right) v u_{xxx} \\ &\quad + \int\int_S v u_{xxxx},\end{aligned} \tag{2.4}$$

and

$$\begin{aligned}\int\int_S u_{yy}v_{yy} &= \left(\int_{\ell_3} - \int_{\ell_4}\right) v_y u_{yy} - \left(\int_{\ell_3} - \int_{\ell_4}\right) v u_{yyy} \\ &\quad + \int\int_S v u_{yyyy}.\end{aligned} \tag{2.5}$$

Similarly, we have

$$\begin{aligned}\int\int_S u_{yy}v_{xx} &= \left(\int_{\ell_1} - \int_{\ell_2}\right) v_x u_{yy} - \left(\int_{\ell_1} - \int_{\ell_2}\right) v u_{xyy} \\ &\quad + \int\int_S v u_{xxyy},\end{aligned} \tag{2.6}$$

and

$$\begin{aligned}\int\int_S u_{xx}v_{yy} &= \left(\int_{\ell_3} - \int_{\ell_4}\right) v_y u_{xx} - \left(\int_{\ell_3} - \int_{\ell_4}\right) v u_{xxy} \\ &\quad + \int\int_S v u_{xxyy}.\end{aligned} \tag{2.7}$$

Also, from integration by parts again we have

$$\begin{aligned}\int\int_S u_{xy}v_{xy} &= \left(\int_{\ell_1} - \int_{\ell_2}\right) v_y u_{xy} - \int\int_S v_y u_{xxy} \\ &= \left(\int_{\ell_1} - \int_{\ell_2}\right) v_y u_{xy} - \left(\int_{\ell_3} - \int_{\ell_4}\right) v u_{xxy} \\ &\quad + \int\int_S v u_{xxyy},\end{aligned} \tag{2.8}$$

where

$$\begin{aligned}&\left(\int_{\ell_1} - \int_{\ell_2}\right) v_y u_{xy} \\ &= [u_{xy}v]_3^4 - [u_{xy}v]_1^2 - \left(\int_{\ell_1} - \int_{\ell_2}\right) v u_{xyy}.\end{aligned} \tag{2.9}$$

After some manipulation, we obtain from Eqs. (2.4)–(2.9)

$$\begin{aligned}\iint_S \Lambda_\mu(u,v) &= \iint_S \{u_{xx}v_{xx}+u_{yy}v_{yy}+\mu(u_{xx}v_{yy}+u_{yy}v_{xx})\\ &\quad +2(1-\mu)u_{xy}v_{xy}\} = \iint_S v\Delta^2 u\\ &\quad +\left(\int_{\ell_1}-\int_{\ell_2}\right)(u_{xx}+\mu u_{yy})v_x\\ &\quad +\left(\int_{\ell_3}-\int_{\ell_4}\right)(u_{yy}+\mu u_{xx})v_y\\ &\quad -\left(\int_{\ell_1}-\int_{\ell_2}\right)(u_{xxx}+(2-\mu)u_{xyy})v\\ &\quad -\left(\int_{\ell_3}-\int_{\ell_4}\right)(u_{yyy}+(2-\mu)u_{xxy})v\\ &\quad +2(1-\mu)([u_{xy}v]_3^4-[u_{xy}v]_1^2)\\ &= \iint_S v\Delta^2 u-\int_{\partial S} m(u)v_n-\int_{\partial S} p(u)v\\ &\quad +2(1-\mu)([u_{xy}v]_3^4-[u_{xy}v]_1^2). \end{aligned} \tag{2.10}$$

This completes the proof of Eq. (2.1).

2.2. Corner effects on polygons

For the rectangular domains in Fig. 1, there do exist the corner terms

$$2(1-\mu)([u_{xy}v]_3^4-[u_{xy}v]_1^2) \tag{2.11}$$

in the Green formulas, which are different from those in Courant and Hilbert [6], p. 252 and Carey and Oden [4], p. 250. In fact, the formulas in Ref. [6] are valid only for the smooth boundary ∂S. There are many papers on Green formulas, see Herrera [9], Gourgeon and Herrera [7], and Russo [29], but only a few reports (e.g. Chien [5]) mention corner effects for biharmonic equations. Below, we will drive the Green formulas by different approaches from Section 2.1 and Chien [5].

Consider a polygon S in Fig. 2, where the boundary $\partial S=\sum_{i=1}^m \Gamma_i$ and Γ_i are straight segments. The corners are denoted by $P_1,P_2,\ldots,P_m$. We have from calculus,

$$\iint_S \Delta u\Delta v=\iint_S(\Delta^2 u)v+\int_{\partial S}(\Delta u)v_n-\int_{\partial S}\frac{\partial(\Delta u)}{\partial n}v, \tag{2.12}$$

and

$$\begin{aligned}&\iint_S(u_{xx}v_{yy}+u_{yy}v_{xx})\\ &=\int_{\partial S}(u_{xx}v_y y_n+u_{yy}v_x x_n)-\iint_S(u_{xxy}v_y+u_{xyy}v_x)\\ &=\int_{\partial S}(u_{xx}v_y y_n+u_{yy}v_x x_n)-\int_{\partial S}u_{xy}(v_y x_n+v_x y_n)+2\iint_S u_{xy}v_{xy},\end{aligned} \tag{2.13}$$

where x_n, y_n and x_s, y_s are the directional cosines of the outward normal and the tangent vectors, respectively.

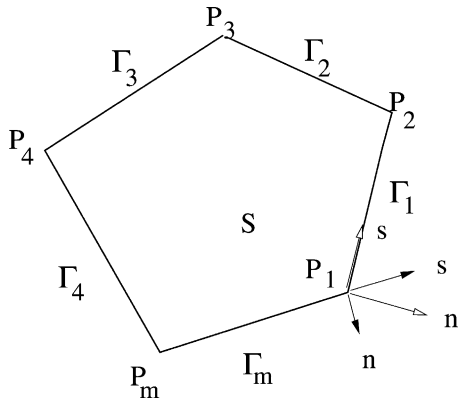

Fig. 2. A polygon with corners.

Since $x_n=y_s$ and $y_n=-x_s$, we obtain

$$\begin{aligned}&\iint_S(2u_{xy}v_{xy}-u_{xx}v_{yy}-u_{yy}v_{xx})\\ &=-\int_{\partial S}(u_{xx}v_y y_n+u_{yy}v_x x_n)+\int_{\partial S}u_{xy}(v_y y_s-v_x x_s).\end{aligned} \tag{2.14}$$

Since x_s, x_n, y_s and y_n on the straight segments Γ_i are constant, we have the following derivative relations

$$\begin{aligned}&v_y=v_n y_n+v_s y_s,\quad v_x=v_n x_n+v_s x_s,\quad u_n=u_x x_n+u_y y_n,\\ &u_s=u_x x_s+u_y y_s,\quad u_{ss}=u_{xx}x_s^2+2u_{xy}x_s y_s+u_{yy}y_s^2,\\ &u_{ns}=u_{xx}x_n x_s+u_{xy}(x_n y_s+x_s y_n)+u_{yy}y_n y_s.\end{aligned} \tag{2.15}$$

Eq. (2.14) is then reduced to

$$\begin{aligned}&\iint_S(2u_{xy}v_{xy}-u_{xx}v_{yy}-u_{yy}v_{xx})\\ &=-\int_{\partial S}(u_{xx}x_s^2+2u_{xy}x_s y_s+u_{yy}y_s^2)v_n+\int_{\partial S}(u_{xx}x_n x_s\\ &\quad +u_{xy}(x_n y_s+x_s y_n)+u_{yy}y_n y_s)\frac{\partial v}{\partial s}\\ &=-\int_{\partial S}u_{ss}v_n+\int_{\partial S}u_{ns}\frac{\partial v}{\partial s}.\end{aligned} \tag{2.16}$$

Next, we have from integral by parts,

$$\begin{aligned}\int_{\partial S}u_{ns}\frac{\partial v}{\partial s}&=\sum_{i=1}^m\int_{\Gamma_i}u_{ns}\frac{\partial v}{\partial s}\\ &=-\sum_{i=1}^m\delta[u_{ns}]_i v_i-\sum_{i=1}^m\int_{\Gamma_i}\left(\frac{\partial}{\partial s}u_{ns}\right)v,\end{aligned} \tag{2.17}$$

where $v_i=v(P_i)$ and $\delta[u_{ns}]_i$ denote the jumps of u_{ns} at corner P_i along the counter clockwise,

$$\delta[u_{ns}]_i=u_{ns}(P_i)|_{\Gamma_i}-u_{ns}(P_i)|_{\Gamma_{i-1}}, \tag{2.18}$$

and $\Gamma_{m+1}=\Gamma_1$. From Eqs. (2.12), (2.16) and (2.17), we obtain the Green formulas,

$$\begin{aligned}
&\iint_S \Lambda_\mu(u,v)=\iint_S \Delta u\Delta v+(1-\mu)\\
&\times\int_{\partial S}(2u_{xy}v_{xy}-u_{xx}v_{yy}-u_{yy}v_{xx})=\iint_S(\Delta^2 u)v\\
&+\int_{\partial S}(\Delta u)v_n-\int_{\partial S}\frac{\partial(\Delta u)}{\partial n}v+(1-\mu)\\
&\times\left\{-\int_{\partial S}u_{ss}v_n-\int_{\partial S}\left(\frac{\partial}{\partial s}u_{ns}\right)v-\sum_{i=1}^{m}\delta[u_{ns}]_i v_i\right\}\\
&=\iint_S v\Delta u^2-\int_{\partial S}(m(v)v_n+p(v)v)\\
&-(1-\mu)\sum_{i=1}^{m}\delta[u_{ns}]_i v_i,
\end{aligned}\tag{2.19}$$

where the general forms of $m(v)$ and $p(v)$ are denoted by [6]

$$\begin{aligned}
m(u)&=-\Delta u+(1-\mu)u_{ss}=-(u_{nn}+\mu u_{ss}),\\
p(u)&=\frac{\partial}{\partial n}\Delta u+(1-\mu)u_{nss}=u_{nnn}+(2-\mu)u_{nss}.
\end{aligned}\tag{2.20}$$

There also exist the corner terms[1] in the Green formulas (2.19),

$$-(1-\mu)\sum_{i=1}^{m}\delta[u_{ns}]_i v_i.\tag{2.21}$$

When the corner angles at P_i in Fig. 2 are just $\pi/2$, and when the second order derivatives are also continuous:

$$u_{ns}(P_i)|_{\Gamma_i}=-u_{ns}(P_i)|_{\Gamma_{i-1}},\tag{2.22}$$

the corner conditions (2.21) are reduced to

$$-(1-\mu)\delta[u_{ns}]_i v_i=2(1-\mu)u_{ns}(P_i)|_{\Gamma_{i-1}}.\tag{2.23}$$

Note that Eq. (2.23) coincides well with Eq. (2.11). Obviously, for the smooth boundary ∂S, the corner terms disappear, and the Green formulas in Ref. [6] are obtained. This shows that the Green formulas in Ref. [6] are the special cases of Eq. (2.19).

Remark 2.1. Let us consider the piecewise curved boundary Γ_i. Denote by $\alpha=\alpha(s)$ the angle between the tangent direction of Γ_i and the x axis, then

$$\begin{aligned}
&x_s=\cos\alpha,\ y_n=-\cos\alpha,\ x_n=y_s=\sin\alpha,\\
&u_n=u_x x_n+u_y y_n=(\sin\alpha)u_x-(\cos\alpha)u_y,\\
&u_s=u_x x_s+u_y y_s=(\cos\alpha)u_x+(\sin\alpha)u_y.
\end{aligned}\tag{2.24}$$

There exist the derivatives of α with respect to $s:\partial\alpha/\partial s=1/\rho$, where ρ denotes the curvature radius of Γ_i, ρ is positive if the curvature center is within S, or negative otherwise. We have from Eq. (2.24) by calculus,

$$\begin{aligned}
u_{ss}&=u_{xx}x_s^2+2u_{xy}x_s y_s+u_{yy}y_s^2-\frac{u_n}{\rho},\\
u_{ns}&=u_{xx}x_n x_s+u_{xy}(x_n y_s+x_s y_n)+u_{yy}y_n y_s+\frac{u_s}{\rho}.
\end{aligned}\tag{2.25}$$

Note that there are two additional terms, $-u_n/\rho$ and u_s/ρ in Eq. (2.25), compared with those in Eq. (2.15).

Similarly, Eq. (2.14) is reduced to

$$\begin{aligned}
&\iint_S(2u_{xy}v_{xy}-u_{xx}v_{yy}-u_{yy}v_{xx})\\
&=-\int_{\partial S}(u_{xx}x_s^2+2u_{xy}x_s y_s+u_{yy}y_s^2)v_n\\
&\quad+\int_{\partial S}(u_{xx}x_n x_s+u_{xy}(x_n y_s+x_s y_n)+u_{yy}y_n y_s)\frac{\partial v}{\partial s}\\
&=-\int_{\partial S}\left(u_{ss}+\frac{u_n}{\rho}\right)v_n+\int_{\partial S}\left(u_{ns}-\frac{u_s}{\rho}\right)\frac{\partial v}{\partial s}\\
&=-\int_{\partial S}\left(u_{ss}+\frac{u_n}{\rho}\right)v_n-\sum_{i=1}^{n}\delta\left[u_{ns}-\frac{u_s}{\rho}\right]_i v_i\\
&\quad-\int_{\partial S}\frac{\partial}{\partial s}\left(u_{ns}-\frac{u_s}{\rho}\right)v.
\end{aligned}\tag{2.26}$$

From Eqs. (2.12) and (2.26), we obtain the Green formulas,

$$\begin{aligned}
&\iint_S\Lambda_\mu(u,v)=\iint_S\Delta u\,\Delta v+(1-\mu)\\
&\times\int_{\partial S}(2u_{xy}v_{xy}-u_{xx}v_{yy}-u_{yy}v_{xx})\\
&=\iint_S v\Delta u^2-\int_{\partial S}(m^*(v)v_n+p^*(v)v)\\
&-(1-\mu)\sum_{i=1}^{m}\delta\left[u_{ns}-\frac{u_s}{\rho}\right]_i v_i,
\end{aligned}\tag{2.27}$$

where

$$\begin{aligned}
m^*(u)&=-\Delta u+(1-\mu)\left(u_{ss}+\frac{u_n}{\rho}\right)\\
&=m(u)+(1-\mu)\frac{u_n}{\rho},\\
p^*(u)&=\frac{\partial}{\partial n}\Delta u+(1-\mu)\left(u_{nss}-\frac{\partial}{\partial s}\left(\frac{u_s}{\rho}\right)\right)\\
&=p(u)-(1-\mu)\frac{\partial}{\partial s}\left(\frac{u_s}{\rho}\right),
\end{aligned}\tag{2.28}$$

and $m(u)$ and $p(u)$ are defined in Eq. (2.20). When natural boundary conditions are subjected to Γ_{i-1} and Γ_i, we obtain

[1] For the curved Γ_i, the additional terms $-(1-\mu)\sum_{i=1}^{m}\delta[u_{ns}-(u_s/\rho)]_i v_i$ are provided by Chien [5], p. 59, see Remark 2.1, where ρ denotes the curvature radius of Γ_i, ρ is positive if the curvature center is within S, or negative otherwise. Obviously, when Γ_i are straight lines, $\rho=\infty$, the corner terms (2.21) are obtained.

the boundary equations

$$m^*(u) = 0, \qquad p^*(u) = 0 \ \text{ on } \Gamma_{i-1} \cup \Gamma_i, \tag{2.29}$$

and the corner conditions

$$\delta\left[u_{ns} - \frac{u_s}{\rho}\right] = 0 \ \text{ at } P_i. \tag{2.30}$$

Eqs. (2.27), (2.29) and (2.30) are given by Chien [5], pp. 245, 238 and 59, respectively. Where Γ_i are straight lines, $\rho = \infty$, Eq. (2.27) leads to Eq. (2.19), and the corner terms $-(1-\mu)\sum_{i=1}^{m} \delta[u_{ns} - (u_s/\rho)]_i v_i$ in Eq. (2.27) to (2.21).

2.3. Boundary conditions for biharmonic equations on polygons

Consider a polygon S, and the exterior boundary conditions on ∂S can be easily derived from the Green formulas. Let the solution $u \in H^2(S)$, where $H^2(S)$ is the Sobolev space defined in Ref. [31]. From $H^2(S)$, the biharmonic solution and its derivatives are continuous on the entire S, i.e. $u \in C^1(S)$. Then the solution of the biharmonic equation, $\Delta^2 u + f = 0$ in S, can be expressed in a weak form: to seek $u \in H^2(S)$ such that

$$\int\int_S \Lambda_\mu(u, v) + \int\int_S fv = 0, \quad v \in H_0^2(S), \tag{2.31}$$

where $H_0^2(S)$ is a subspace of $H^2(S)$ satisfying suitable homogeneous boundary conditions for v. Based on the Green formulas in Section 2.1,

$$0 = \int\int_S (\Delta^2 u + f)v - \int_{\partial S} (m(u)v_n + p(u)v) + 2(1 - \mu)([u_{xy}v]_3^4 - [u_{xy}v]_1^2), \tag{2.32}$$

we obtain three equations from an arbitrary function v,

$$\int\int_S (\Delta^2 u + f)v = 0, \tag{2.33}$$

$$\int_{\partial S} (m(u)v_n + p(u)v) = 0, \tag{2.34}$$

$$2(1-\mu)([u_{xy}v]_3^4 - [u_{xy}v]_1^2) = 0. \tag{2.35}$$

Since v in S is arbitrary, we obtain the biharmonic equation, $\Delta^2 u + f = 0$ in S from Eq. (2.33), where f also represents the exterior surface force. Next, let us consider different exterior boundary conditions. For the clamped condition: $u = g_1$ and $u_n = g_2$ on ∂S, in view of $v = 0$ and $v_n = 0$ on ∂S, we can see that the boundary integrals satisfy Eq. (2.34) automatically. Next, for the simply supported condition $u = g_1$, since v_n on ∂S is arbitrary, then the additional condition, the boundary blending moment $m(u) = 0$ on ∂S, is obtained from Eq. (2.34). For the special case: $u =$ constant, we have $u_{ss} = 0$, which gives $m(u) = -u_{nn} - \mu u_{ss} = -u_{nn} = 0$. Hence we obtain a concise form of the simply supported conditions: $u =$ constant and $u_{nn} = 0$ on ∂S.

For symmetric conditions, $u_n = 0$ on ∂S, we have the additional condition: $p(u) = u_{nnn} + (2-\mu)u_{nss} = 0$ from Eq. (2.34). Since $u_{nss} = 0$ on ∂S, $p(u) = 0$ is also simplified to $u_{nnn} = 0$ on ∂S. So we obtain the symmetric conditions: $u_n = u_{nnn} = 0$ on ∂S. For the simple natural boundary condition, e.g. no constraints are given on ∂S, then $m(u) = 0$ and $p(u) = 0$ from Eq. (2.34). Suppose that the natural boundary conditions are given by the exterior boundary force $p(u) = g_3$ and the bending moment $m(u) = g_4$ on Γ_N, where Γ_N is a partial of ∂S, and the clamped boundary condition is subjected on $\partial S \backslash \Gamma_N$. The unique solution of biharmonic equations is then expressed: to seek $u \in H^2(S)$ such that

$$\int\int_S \Lambda_\mu(u, v) + \int\int_S fv + \int_{\Gamma_N} (g_3 v + g_4 v_n) = 0, \quad v \in H_0^2(S). \tag{2.36}$$

We may consider mixed types of different boundary conditions, where different conditions are given on different edges of ∂S. In this case, the corner terms must be considered for the natural corners, where two adjacent edges are *all* subjected to the natural conditions. Since v is arbitrary, we obtain the corner condition $u_{xy} = 0$ from Eq. (2.35), which is important for the collocation Trefftz method, see Section 3.3, because all boundary conditions including the corner conditions must be satisfied as best as possible. Moreover, the corner condition $u_{xy}v = 0$ is satisfied automatically, if one adjacent edge of the corner is subjected to (1) the clamped condition, (2) the symmetric condition, or (3) the simply supported condition with $u_n =$ constant. It is easy to see that either $v = 0$ or $u_{ns} = u_{xy} = 0$ on one edge yields $u_{xy}v = 0$ automatically at the corner.

We may discuss the uniqueness of the solutions by considering the homogeneous biharmonic equation $\Delta^2 u = 0$. A solution u can be also described as the minimal energy:

$$E(u) = \min_{v \in H_0^2(S)} E(v), \tag{2.37}$$

where

$$E(v) = \frac{1}{2}\int\int_S \Lambda_\mu(v, v) = \frac{1}{2}\int\int_S \mu(v_{xx}^2 + v_{yy}^2) + (1-\mu)(v_{xx}^2 + v_{yy}^2 + 2v_{xy}^2). \tag{2.38}$$

When $0 \le \mu < 1$, condition $E(v) = 0$ leads to that $v_{xx} = v_{yy} = v_{xy} = 0$, then the linear functions are obtained, i.e. $v = a + bx + cy$ with constants a, b and c. To guarantee the unique solutions, the linear functions must be zero: $v = a + bx + cy \equiv 0$. For the mixed types of boundary conditions, there exist unique solutions for one edge, e.g. $\overline{AB}$ in Fig. 3, subjected to the clamped boundary condition. Since

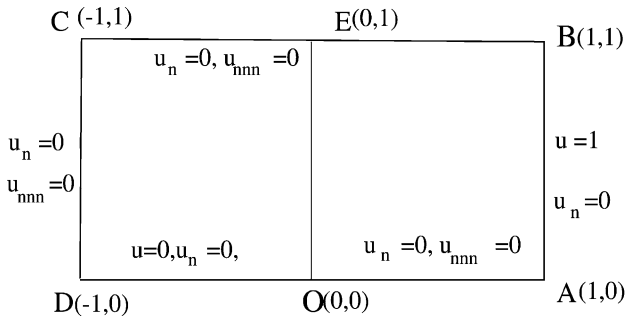

Fig. 3. The boundary conditions of biharmonic equations for Model I.

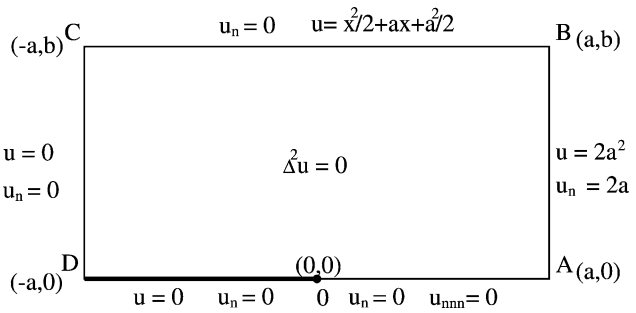

Fig. 5. The boundary conditions of biharmonic equations for Model III.

v_n (e.g. v_x) $= v = 0$ on $\overline{AB}$, then the constants $b = 0$ and $(a + cy)|_{x=1} = 0$. So $a = c = 0$ and then $v \equiv 0$. This confirms the unique solutions if one edge of a corner is subjected to the clamped boundary condition.

In summary, we have derived five typical boundary conditions for biharmonic equations on polygonal domains:

1. The symmetric condition: $u_n = 0$, $u_{nnn} = 0$.
2. The clamped condition: $u = c_0$, $u_n = c_1$.
3. The simply supported condition: $u = c_0$, $u_{nn} = c_2$.
4. The natural condition: $m(u) = -u_{nn} - \mu u_{ss} = c_3$, $p(u) = u_{nnn} + (2 - \mu)u_{nss} = c_4$. Here c_i are the given constants, which are dependent on the problems to be solved.
5. The natural corner condition: $u_{xy} = 0$.

Note that for biharmonic equations, the interior and exterior boundary conditions and the corner conditions are important not only to the collocation Trefftz method but also to the collocation methods using the radial basis functions, or the Sinc functions, etc.

3. The collocation Trefftz methods

3.1. Three crack models

Consider the homogeneous biharmonic equation

$$\Delta^2 u = 0 \quad \text{in } S, \tag{3.1}$$

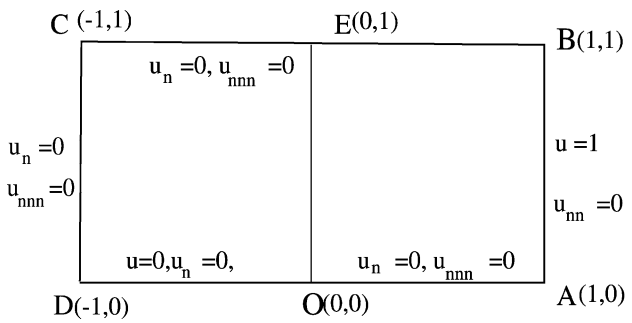

Fig. 4. The boundary conditions of biharmonic equations for Model II.

where the solution domain is the rectangle: $S = \{(x, y), -1 < x < 1, 0 < y < 1\}$. In this paper, we study three crack models of singularity problems, shown in Figs. 3–5. The section $\overline{OD}$ represents an interior crack under the clamped condition $u = u_n = 0$. From Section 2.3, the symmetric conditions, $u_n = u_{nnn} = 0$ on $\overline{OA} \cup \overline{BC} \cup \overline{CD}$, are required. Here n is the outward normal direction to the boundary ∂S. On $\overline{AB}$, when the clamped conditions are provided, we propose the biharmonic boundary value problem with the following conditions, called Model I in this paper, see Fig. 3:

$$u|_{\overline{OD}} = 0, \qquad u_y|_{\overline{OD}} = 0, \tag{3.2}$$

$$u_y|_{\overline{OA}} = 0, \qquad u_{yyy}|_{\overline{OA}} = 0, \tag{3.3}$$

$$u|_{\overline{AB}} = 1, \qquad u_x|_{\overline{AB}} = 0, \tag{3.4}$$

$$u_y|_{\overline{BC}} = 0, \qquad u_{yyy}|_{\overline{BC}} = 0, \tag{3.5}$$

$$u_x|_{\overline{CD}} = 0, \qquad u_{xxx}|_{\overline{CD}} = 0. \tag{3.6}$$

We may replace the clamped condition on $\overline{AB}$ by the simply supported condition,

$$u|_{\overline{AB}} = 1, \qquad u_{xx}|_{\overline{AB}} = 0, \tag{3.7}$$

but the other boundary conditions remain the same as those in Model I. Such a model is called Model II, see Fig. 4. Note that Models I and II resemble the Motz's problem in Refs. [20,26].

Next, we choose the models by Schiff et al. [30] with all the clamped conditions on ∂S, see Fig. 5,

$$\Delta^2 u = 0, \quad \text{on } S, \tag{3.8}$$

$$u|_{\overline{OD}} = 0, \qquad u_y|_{\overline{OD}} = 0, \tag{3.9}$$

$$u_y|_{\overline{OA}} = 0, \qquad u_{yyy}|_{\overline{OA}} = 0, \tag{3.10}$$

$$u|_{\overline{AB}} = 2a^2, \qquad u_x|_{\overline{AB}} = 2a, \tag{3.11}$$

$$u|_{\overline{BC}} = \frac{x^2}{2} + ax + \frac{a^2}{2}, \qquad u_y|_{\overline{BC}} = 0, \tag{3.12}$$

$$u|_{\overline{CD}} = 0, \qquad u_x|_{\overline{CD}} = 0, \tag{3.13}$$

where $S = \{(x, y), -a < x < a, 0 < y < b\}$. When parameters $a = b = 1$, the model (3.8)–(3.13) is called Model III in this paper.

For the clamped crack on $\overline{OD}$, the particular solutions of these models are known, and given by Schiff et al. [30]:

$$u = \sum_{i=1}^{\infty} (d_i \phi_i(r,\theta) + c_i f_i(r,\theta)), \tag{3.14}$$

where d_i and c_i are expansion coefficients, and the singular particular solutions are

$$\phi_i(r,\theta) = r^{i+(1/2)} \left\{ \cos\left(i - \frac{3}{2}\right)\theta - \frac{i-\frac{3}{2}}{i+\frac{1}{2}} \cos\left(i + \frac{1}{2}\right)\theta \right\}, \tag{3.15}$$

and the analytic particular solutions

$$f_i(r,\theta) = r^{i+1}\{\cos(i-1)\theta - \cos(i+1)\theta\}. \tag{3.16}$$

3.2. Description of the method

Take Model I as an example and describe the collocation Trefftz method, since the algorithms of the collocation Trefftz method for other models may be similarly described. Choose finite terms of particular solutions

$$u_N = \sum_{i=1}^{N} (\tilde{d}_i \phi_i(r,\theta) + \tilde{c}_i f_i(r,\theta)), \tag{3.17}$$

where $\tilde{d}_i$ and $\tilde{c}_i$ are approximate coefficients to be sought. Since the particular solutions (3.15) and (3.16) satisfy the biharmonic equation (3.1) in S and the boundary conditions on $\overline{OD}$ and $\overline{OA}$ already, the unknown coefficients $\tilde{c}_i$ and $\tilde{d}_i$ can be obtained by satisfying the rest of boundary conditions as best as possible.

For Model I, there exists the crack point at O. We split S into S^+ and S^-, where $S^+ = S \cap (x \geq 0)$ and $S^- = S \cap (x \leq 0)$. Then the Green formulas are applied to S^+ and S^- in Fig. 3, to give

$$\begin{aligned} \int\int_S \Lambda_\mu(u,v) &= \int\int_{S^+} \Lambda_\mu(u,v) + \int\int_{S^-} \Lambda_\mu(u,v) \\ &= \int\int_S v\Delta^2 u - \int_{\partial S} (m(u)v_n + p(u)v) + 2(1-\mu) \\ &\quad \times ([u_{xy}v]_A^B - [u_{xy}v]_{O^+}^E + [u_{xy}v]_{O^-}^E - [u_{xy}v]_D^C), \end{aligned} \tag{3.18}$$

where point $E = (0,1)$. From Eqs. (3.2)–(3.6), we obtain

$$v(A) = v(B) = v(D) = v(O^-) = 0,$$

$$u_{xy}(C) = u_{xy}(E) = u_{xy}(O^+) = 0.$$

Hence, the last term on the right hand side of Eq. (3.18) is zero automatically. In this case, the corner conditions at E and O may not be needed in the collocation Trefftz method, either. We confirm again the boundary conditions given in Eqs. (3.2)–(3.6).

For Model I with the boundary conditions (3.2)–(3.6), define an energy on the boundary by

$$\begin{aligned} I(v) &= I(d_i, c_i) \\ &= \int_{\overline{AB}} ((v-1)^2 + w_1^2 v_x^2) + \int_{\overline{BC}} (w_1^2 v_y^2 + w_3^2 v_{yyy}^2) \\ &\quad + \int_{\overline{CD}} (w_1^2 v_x^2 + w_3^2 v_{xxx}^2), \end{aligned} \tag{3.19}$$

where the weights $w_i = 1/(N+1)^i$, based on the analysis in Refs. [20,23]. The approximate coefficients $\tilde{d}_i$ and $\tilde{c}_i$ can be found by

$$I(u_N) = I(\tilde{d}_i, \tilde{c}_i) = \min_{d_i, c_i} I(d_i, c_i). \tag{3.20}$$

To be more precise, we use the simplest midpoint rule to discretize the integrals in Eq. (3.19), where the uniform partitions are chosen for $\overline{AB} \cup \overline{BC} \cup \overline{CD}$, and the division number of $\overline{AB}$ is denoted by M. This is equivalent to the direct collocation method to establish the linear algebraic equations,

$$\mathbf{F}\vec{x} = \vec{b}, \tag{3.21}$$

where $\vec{x}$ consists of $2N$ coefficients $\tilde{d}_i$ and $\tilde{c}_i$, and $\mathbf{F}$ is the $8M \times 2N$ matrix. Choose $8M \gg 2N$, and the least squares solution is just the solution $\vec{x}$, e.g. the coefficients $\tilde{d}_i$ and $\tilde{c}_i$.

In computation, we use the error notation for accuracy,

$$E_2 = \|\epsilon\|_B = \|u - v\|_B = \sqrt{I(v)}, \tag{3.22}$$

and the condition number for stability

$$\text{Cond.} = \left\{ \frac{\lambda_{\max}(\mathbf{F}^{\mathrm{T}}\mathbf{F})}{\lambda_{\min}(\mathbf{F}^{\mathrm{T}}\mathbf{F})} \right\}^{1/2}, \tag{3.23}$$

where $\lambda_{\max}(\mathbf{A})$ and $\lambda_{\min}(\mathbf{A})$ are the maximal and minimal eigenvalues of the matrix $\mathbf{A} = \mathbf{F}^{\mathrm{T}}\mathbf{F}$.

3.3. The collocation Trefftz method with natural corners

Let the clamped and the natural conditions be given on $\overline{AB}$ and $\overline{BC} \cup \overline{CD}$ in Fig. 3, respectively,

$$\begin{aligned} &u = 1, \quad u_n = 0, \quad \text{on } \overline{AB}; \\ &m(u) = p(u) = 0 \quad \text{on } \overline{BC} \cup \overline{CD}. \end{aligned} \tag{3.24}$$

Since point C is a natural corner, the corner condition is needed: $u_{xy}(C) = 0$. The collocation Trefftz method involving the natural corner C is given by

$$I^*(u_N) = I^*(\tilde{d}_i, \tilde{c}_i) = \min_{d_i, c_i} I^*(d_i, c_i), \tag{3.25}$$

where

$$\begin{aligned} I^*(v) &= \int_{\overline{AB}} ((v-1)^2 + w_1^2 v_n^2) + \int_{\overline{BC} \cup \overline{CD}} (w_2^2 m^2(v) \\ &\quad + w_3^2 p^2(v)) + 2(1-\mu) w_2^2 v_{xy}^2(C), \end{aligned} \tag{3.26}$$

and the weights are $w_i = 1/(N+1)^i$. Note that the corner term involving $v_{xy}^2(C)$ is *necessary* to the collocation Trefftz method for the biharmonic equations with natural corners. When the corner angles at $\angle DCB$ is not just $\pi/2$, the corner contribution in Eq. (3.26) is replaced by $(1-\mu)w_2^2(v_{ns}^+(C) - v_{ns}^-(C))^2$ based on the analysis in Section 2.2.

3.4. Formulas of partial derivatives

In this section, we provide useful derivative formulas for u_x, u_y, u_{xx}, u_{yy}, u_{xy}, u_{xxx}, u_{yyy}, u_{xxy} and u_{xyy}, which are required by the collocation Trefftz method. Since the particular solutions (3.15) and (3.16) in S are given in polar coordinates, we will find their explicit formulas of partial derivatives with respect to x and y. Let the origins of the Cartesian and polar coordinates be the same, we obtain

$$\begin{aligned} u_x &= \cos\theta\frac{\partial u}{\partial r} - \sin\theta\frac{\partial u}{r\partial\theta}, \\ u_y &= \sin\theta\frac{\partial u}{\partial r} + \cos\theta\frac{\partial u}{r\partial\theta}. \end{aligned} \tag{3.27}$$

Based on Eq. (3.27), we have

$$\begin{aligned} u_{xx} &= \left(\cos\theta\frac{\partial}{\partial r} - \sin\theta\frac{\partial}{r\partial\theta}\right)\left(\cos\theta\frac{\partial}{\partial r} - \sin\theta\frac{\partial}{r\partial\theta}\right)u \\ &= \cos^2\theta\frac{\partial^2 u}{\partial r^2} - \sin 2\theta\left(\frac{\partial}{r\partial r}\frac{\partial u}{\partial\theta} - \frac{\partial u}{r^2\partial\theta}\right) + \frac{\sin^2\theta}{r}\frac{\partial u}{\partial r} \\ &\quad + \frac{\sin^2\theta}{r^2}\frac{\partial^2 u}{\partial\theta^2}. \end{aligned} \tag{3.28}$$

Similarly, we have

$$\begin{aligned} u_{yy} &= \sin^2\theta\frac{\partial^2 u}{\partial r^2} + \sin 2\theta\left(\frac{\partial}{r\partial r}\frac{\partial u}{\partial\theta} - \frac{\partial u}{r^2\partial\theta}\right) \\ &\quad + \frac{\cos^2\theta}{r}\frac{\partial u}{\partial r} + \frac{\cos^2\theta}{r^2}\frac{\partial^2 u}{\partial\theta^2}, \end{aligned} \tag{3.29}$$

and

$$\begin{aligned} u_{xy} &= \cos\theta\sin\theta\frac{\partial^2 u}{\partial r^2} + \frac{\cos^2\theta}{r}\frac{\partial}{\partial r}\frac{\partial u}{\partial\theta} - \frac{\cos^2\theta}{r^2}\frac{\partial u}{\partial\theta} \\ &\quad - \frac{\sin^2\theta}{r}\frac{\partial}{\partial r}\frac{\partial u}{\partial\theta} - \frac{\cos\theta\sin\theta}{r}\frac{\partial u}{\partial r} \\ &\quad - \frac{\cos\theta\sin\theta}{r^2}\frac{\partial^2 u}{\partial\theta^2} + \frac{\sin^2\theta}{r^2}\frac{\partial u}{\partial\theta}. \end{aligned} \tag{3.30}$$

After some manipulation, we can also obtain

$$\begin{aligned} u_{xxx} &= \left(\cos\theta\frac{\partial}{\partial r} - \sin\theta\frac{\partial}{r\partial\theta}\right) \\ &\quad \times\left[\cos^2\theta\frac{\partial^2}{\partial r^2} - \sin 2\theta\left(\frac{\partial}{r\partial r}\frac{\partial}{\partial\theta} - \frac{\partial}{r^2\partial\theta}\right)\right. \\ &\quad \left. + \frac{\sin^2\theta}{r}\frac{\partial}{\partial r} + \frac{\sin^2\theta}{r^2}\frac{\partial^2}{\partial\theta^2}\right]u \\ &= \cos^3\theta\frac{\partial^3 u}{\partial r^3} - \frac{3\cos\theta\sin 2\theta}{2r}\frac{\partial^2}{\partial r^2}\frac{\partial u}{\partial\theta} \\ &\quad + \frac{3\sin\theta\sin 2\theta}{2r^2}\frac{\partial}{\partial r}\frac{\partial^2 u}{\partial\theta^2} - \frac{\sin^3\theta}{r^3}\frac{\partial^3 u}{\partial\theta^3} \\ &\quad + \frac{3\sin\theta\sin 2\theta}{2r}\frac{\partial^2 u}{\partial r^2} - \frac{3(\sin\theta - 3\sin 3\theta)}{4r^2} \\ &\quad \times\frac{\partial}{\partial r}\frac{\partial u}{\partial\theta} - \frac{3\sin\theta\sin 2\theta}{r^3}\frac{\partial^2 u}{\partial\theta^2} \\ &\quad - \frac{3\sin\theta\sin 2\theta}{2r^2}\frac{\partial u}{\partial r} - \frac{2\sin 3\theta}{r^3}\frac{\partial u}{\partial\theta}. \end{aligned} \tag{3.31}$$

Other derivatives of third order are given by

$$\begin{aligned} u_{yyy} &= \sin^3\theta\frac{\partial^3 u}{\partial r^3} + \frac{3\sin\theta\sin 2\theta}{2r}\frac{\partial^2}{\partial r^2}\frac{\partial u}{\partial\theta} \\ &\quad + \frac{3\cos\theta\sin 2\theta}{2r^2}\frac{\partial}{\partial r}\frac{\partial^2 u}{\partial\theta^2} + \frac{\cos^3\theta}{r^3}\frac{\partial^3 u}{\partial\theta^3} \\ &\quad + \frac{3\cos\theta\sin 2\theta}{2r}\frac{\partial^2 u}{\partial r^2} + \frac{3(\cos\theta + 3\cos 3\theta)}{4r^2}\frac{\partial}{\partial r}\frac{\partial u}{\partial\theta} \\ &\quad - \frac{3\cos\theta\sin 2\theta}{r^3}\frac{\partial^2 u}{\partial\theta^2} - \frac{3\cos\theta\sin 2\theta}{2r^2}\frac{\partial u}{\partial r} - \frac{2\cos 3\theta}{r^3}\frac{\partial u}{\partial\theta}, \\ u_{xxy} &= \sin\theta\cos^2\theta\frac{\partial^3 u}{\partial r^3} + \frac{\cos\theta + 3\cos 3\theta}{4r}\frac{\partial^2}{\partial r^2}\frac{\partial u}{\partial\theta} \\ &\quad + \frac{\sin\theta - 3\sin 3\theta}{4r^2}\frac{\partial}{\partial r}\frac{\partial^2 u}{\partial\theta^2} + \frac{\sin\theta\sin 2\theta}{2r^3}\frac{\partial^3 u}{\partial\theta^3} \\ &\quad + \frac{\sin\theta - 3\sin 3\theta}{4r}\frac{\partial^2 u}{\partial r^2} + \frac{\cos\theta - 9\cos 3\theta}{4r^2}\frac{\partial}{\partial r}\frac{\partial u}{\partial\theta} \\ &\quad - \frac{2\sin\theta - 3\sin 3\theta}{2r^3}\frac{\partial^2 u}{\partial\theta^2} - \frac{\sin\theta - 3\sin 3\theta}{4r^2}\frac{\partial u}{\partial r} \\ &\quad + \frac{2\cos 3\theta}{r^3}\frac{\partial u}{\partial\theta}, \end{aligned} \tag{3.32}$$

and

$$u_{xyy}=\cos\theta\sin^2\theta\frac{\partial^3 u}{\partial r^3}+\frac{3\sin 3\theta-\sin\theta}{4r}\frac{\partial^2}{\partial r^2}\frac{\partial u}{\partial\theta}+\frac{\cos\theta+3\cos 3\theta}{4r^2}\frac{\partial}{\partial r}\frac{\partial^2 u}{\partial\theta^2}-\frac{\sin\theta\cos^2\theta}{r^3}\frac{\partial^3 u}{\partial\theta^3}+\frac{\cos\theta+3\cos 3\theta}{4r}\frac{\partial^2 u}{\partial r^2}-\frac{\sin\theta+9\sin 3\theta}{4r^2}\frac{\partial}{\partial r}\frac{\partial u}{\partial\theta}-\frac{\cos\theta+3\cos 3\theta}{2r^3}\frac{\partial^2 u}{\partial\theta^2}-\frac{\cos\theta+3\cos 3\theta}{4r^2}\frac{\partial u}{\partial r}+\frac{2\sin 3\theta}{r^3}\frac{\partial u}{\partial\theta}. \tag{3.33}$$

In the computation of Eqs. (3.27)–(3.33), the derivatives of u with respect to r and θ can be easily obtained directly from Eqs. (3.15) and (3.16). For the analytical particular solutions $f_i(r,\theta)$ in Eq. (3.16), the explicit derivatives, $u_x, u_y, \ldots, u_{xyy}$, can be derived straightforward. However, for the singular particular solutions, $\phi_i(r,\theta)$ in Eq. (3.15), the above computational formulas are *essential* in computations.

4. The collocation Trefftz method with interior boundary

4.1. Interior continuity conditions on interfaces

For simplicity, let $S=S^+\cup S^-$, where S, S^+ and S^- are all polygons, shown in Fig. 6. The interface is a straight line, denoted by $\Gamma_0=\overline{EO}$. Suppose that the particular solutions $u^\pm$ satisfy $\Delta^2 u^\pm=f$ in $S^\pm$. Also let the clamped and the natural conditions be enforced on $\overline{CD}\cup\overline{DA}\cup\overline{AB}$ and $\overline{BC}$, respectively. We will derive the interior continuity conditions on the interface:

$$u^+=u^-,\quad u_n^+=u_n^-,\quad u_{nn}^+=u_{nn}^-,\quad u_{nnn}^+=u_{nnn}^-,\ \text{on}\ \Gamma_0, \tag{4.1}$$

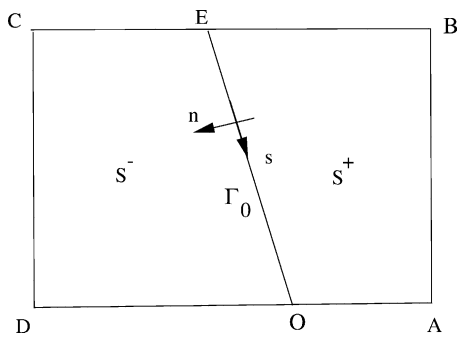

Fig. 6. An interior boundary.

where n is the outnormal to ∂S^+. By applying the Green formulas to S^+ and S^-, we have

$$\iint_{S^+}\Lambda_\mu(u,v)=\iint_{S^+}v\Delta^2 u-\int_{\partial S^+}(m(u)v_n+p(u)v)+2(1-\mu)((u_{ns}^+v)(E)-(-u_{xy}^+v)(E)),$$

$$\iint_{S^-}\Lambda_\mu(u,v)=\iint_{S^-}v\Delta^2 u-\int_{\partial S^-}(m(u)v_n+p(u)v)+2(1-\mu)((-u_{ns}^-v)(E)-(u_{xy}^-v)(E)),$$

where s is the tangent direction in Fig. 6, and $m(u)$ and $p(u)$ are defined in Eq. (2.3). For the given boundary conditions, we obtain

$$\begin{aligned}0&=\iint_{S^+}\Lambda_\mu(u,v)+\iint_{S^-}\Lambda_\mu(u,v)-\iint_S fv\\&=\iint_S v(\Delta^2 u-f)-\int_{\Gamma_0}\{(m(u^+)v_n^+-m(u^-)v_n^-)\\&\quad+(p(u^+)v^+-p(u^-)v^-)\}+2(1-\mu)\{(u_{ns}^++u_{xy}^+)v(E^+)\\&\quad-(u_{ns}^-+u_{xy}^-)v(E^-)\}.\end{aligned} \tag{4.2}$$

Since $u,\ v\in C^1(S)$ we have the first continuity conditions:

$$u^+=u^-,\quad u_n^+=u_n^-\ \text{on}\ \Gamma_0. \tag{4.3}$$

Then the boundary integrals in Eq. (4.2) are expressed as

$$\int_{\Gamma_0}\{(m(u^+)-m(u^-))v_n+(p(u^+)-p(u^-))v\}=0. \tag{4.4}$$

Since v and v_n are arbitrary on Γ_0, we obtained the second continuity conditions:

$$m(u^+)=m(u^-),\quad p(u^+)=-p(u^-)\ \text{on}\ \Gamma_0. \tag{4.5}$$

From Eq. (4.3) we have $u_{ss}^+=u_{ss}^-$ and $u_{nss}^+=u_{nss}^-$ on Γ_0. The above conditions (4.5) are then simplified to

$$u_{nn}^+=u_{nn}^-,\quad u_{nnn}^+=u_{nnn}^-,\ \text{on}\ \Gamma_0. \tag{4.6}$$

Hence, by noting Eqs. (2.2) and (2.3), we have derived the interior continuity conditions in Eq. (4.1).

Next, consider the boundary point condition at E. Since $u\in C^1(S)$ and $v(E)(=v(E^+)=v(E^-))$ is arbitrary, from Eq. (4.2) we also obtain the boundary point conditions,

$$u_{ns}^++u_{xy}^+=u_{ns}^-+u_{xy}^-\ \text{at}\ E. \tag{4.7}$$

Suppose that second order derivatives of u are continuous far from the singular points. The first two equalities in Eq. (4.1) lead to $u_{ss}^+=u_{ss}^-$ and $u_{ns}^+=u_{ns}^-$ at E, which with $u_{nn}^+=u_{nn}^-$ at E give Eq. (4.7) automatically. Hence the point continuity condition at E is unnecessary for this interface problem. Such a conclusion is also valid for other kinds of boundary conditions on $\overline{BC}$. A similar analysis can be made for the interface problems where two interior boundaries are

intersected at an interior point $E \in S$. The same continuity interior conditions (4.1) on Γ_0 are obtained, but the interior intersection E may become a singular point which must be considered carefully [22].

4.2. Description of the collocation Trefftz method

Let the solution domain S be divided into three subdomains S_0, S_1 and S_2 shown in Fig. 7. The polar coordinates at three corners O, B and C are (r, θ), (ξ, ϕ) and (η, ψ), respectively. The piecewise particular solutions of Model I are given explicitly by

$$u_N = \sum_{i=1}^{N} \left\{ d_i r^{i+(1/2)} \left(\cos\left(i - \frac{3}{2}\right)\theta - \frac{i-\frac{3}{2}}{i+\frac{1}{2}} \cos\left(i + \frac{1}{2}\right)\theta \right) + c_i r^{i+1} (\cos(i-1)\theta - \cos(i+1)\theta) \right\}, \ (r,\theta) \in S_0, \tag{4.8}$$

$$u_M = 1 + \sum_{i=1}^{M} \{ a_i \xi^{2i} (\cos(2i-2)\phi + \cos 2i\phi) + b_i \xi^{2i+1} (\cos(2i-1)\phi + \frac{2i-1}{2i+1} \cos(2i+1)\phi \}, \ (\xi,\phi) \in S_1, \tag{4.9}$$

$$u_K = \sum_{i=1}^{K} a_i^* \eta^{2i} \{ \cos(2i-2)\psi + \cos 2i\psi \}, \ (\eta,\psi) \in S_2, \tag{4.10}$$

where d_i, c_i, a_i, b_i and a_i^* are expansion coefficients to be sought. For Model II, the particular solutions in S_1 are replaced by:

$$u_M = 1 + \sum_{i=1}^{M} a_i \xi^{2i} (\cos(2i-2)\phi + \cos 2i\phi), \ (\xi,\phi) \in S_1, \tag{4.11}$$

and the other solutions u_N and u_K remain the same as those in Eqs. (4.8) and (4.10). Note that for Model I, the piecewise particular solutions (4.8)–(4.10) satisfy the biharmonic equation in S and all the exterior boundary conditions on ∂S.

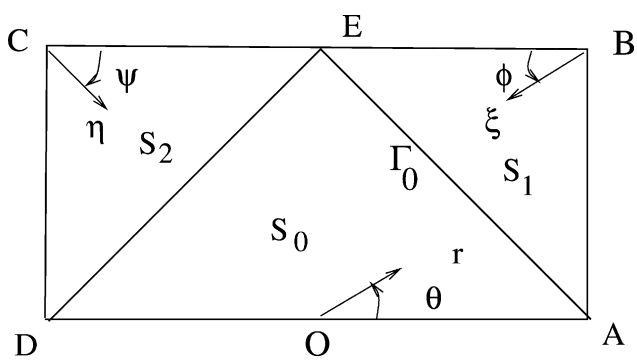

Fig. 7. Partition of S by the interior boundary Γ_0.

The piecewise solutions must match the following interior continuity boundary conditions, based on Section 4.1

$$u^+ = u^-, \quad u_n^+ = u_n^-, \quad u_{nn}^+ = u_{nn}^-, \quad u_{nnn}^+ = u_{nnn}^-, \ \text{on } \Gamma_0, \tag{4.12}$$

where $u^+ = u|_{S_0}$ and $u^- = u|_{S_1 \cup S_2}$. Denote the interior boundary $\Gamma_0 = \overline{AE} \cup \overline{DE}$ and define the energy

$$I(v) = I(d_i, c_i, a_i, b_i, a_i^*) = \int_{\Gamma_0} \{ (v^+ - v^-)^2 + w_1^2 (v_n^+ - v_n^-)^2 + w_2^2 (v_{nn}^+ - v_{nn}^-)^2 + w_3^2 (u_{nnn}^+ - v_{nnn}^-)^2 \}, \tag{4.13}$$

where $w_i = 1/(\max\{N+1, 2M, 2K\})^i$. Hence the solution of the collocation Trefftz method with interior boundary Γ_0 can be described as

$$I(u_{N,M,K}) = I(\tilde{d}_i, \tilde{c}_i, \tilde{a}_i, \tilde{b}_i, \tilde{a}_i^*) = \min_{\forall d_i, c_i, a_i, b_i, a_i^*} I(v), \tag{4.14}$$

where the admissible functions are given in Eqs. (4.8)–(4.10).

The interior boundary Γ_0 consists of two straight line segments $\overline{DE}$ and $\overline{AE}$, with angles $\Theta = \frac{1}{4}\pi$ and $\Theta = -\frac{1}{4}\pi$ to the y axis, respectively, see Fig. 7. To carry out the collocation Trefftz method in Eq. (4.14) we need the derivative formulas u_n, u_{nn} and u_{nnn}. From the following arguments, we may simply use the derivatives formulas of u_x, u_y, etc. in Section 3.4, by replacing θ with $\theta - \Theta$.

In fact, we have for $\Gamma_0 (= \overline{AE})$ in Fig. 8,

$$\frac{\partial u}{\partial n} = \frac{\partial u}{\partial r} \cos(n, r) + \frac{\partial u}{r \partial \theta} \cos(n, \theta), \quad \frac{\partial u}{\partial s} = \frac{\partial u}{\partial r} \cos(s, r) + \frac{\partial u}{r \partial \theta} \cos(s, \theta), \tag{4.15}$$

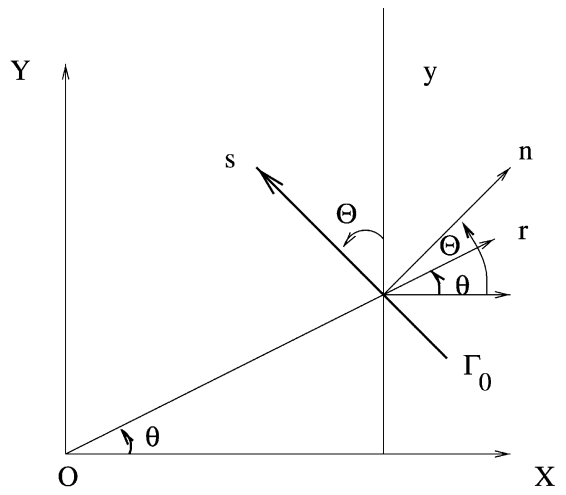

Fig. 8. The normal and tangent directions of Γ_0.

where

$$\begin{aligned}
&\cos(n,r)=\cos(\theta-\Theta),\\
&\cos(n,\theta)=\cos\left(\frac{1}{2}\pi+\Theta-\theta\right)=-\sin(\theta-\Theta),\\
&\cos(s,r)=\cos\left(\frac{1}{2}\pi-(\theta-\Theta)\right)=\sin(\theta-\Theta),\\
&\cos(s,\theta)=\cos(\theta-\Theta).
\end{aligned}\tag{4.16}$$

Hence we have

$$\frac{\partial u}{\partial n}=\frac{\partial u}{\partial r}\cos(\theta-\Theta)-\frac{\partial u}{r\partial\theta}\sin(\theta-\Theta),\tag{4.17}$$

$$\frac{\partial u}{\partial s}=\frac{\partial u}{\partial r}\sin(\theta-\Theta)+\frac{\partial u}{r\partial\theta}\cos(\theta-\Theta),\tag{4.18}$$

where $\Theta=\pm\frac{1}{4}\pi$. Note that when $\Theta=0$, we obtain u_x and u_y in Eq. (3.27) from Eqs. (4.17) and (4.18). Therefore, we may directly obtain the corresponding formulas from Section 3.4 by replacing θ with $\theta-\Theta$.

5. Error bounds

For simplicity, we consider the collocation Trefftz method for Model I in Fig. 3. Let $S=S_1\cup S_2$, where $S_1=S\cap(x<0)$ and $S_2=S\cap(x>0)$. We have the Green formulas for $v=u_N$, Γ

$$\begin{aligned}
\int\int_S \Lambda_\mu(v,v)=&\int\int_S v\Delta^2 v-\int_{\partial S}m(v)v_n-\int_{\partial S}p(v)v\\
&+2(1-\mu)\{[v_{xy}v]_A^B-[v_{xy}v]_{O^+}^E+[v_{xy}v]_{O^-}^E\\
&-[v_{xy}v]_D^C\},
\end{aligned}\tag{5.1}$$

where $E=(0,1)$, $m(v)=-v_{nn}$ and $p(v)=v_{nnn}$ on $\overline{AB}\cup\overline{BC}\cup\overline{CD}$ for Model I. Hence for the particular solutions v of biharmonic equations, since $v|_D=v|_{O^-}=0$ and $v_{xy}|_A=v_{xy}|_{O^+}=0$ for $v=v_N$, the Green formulas are simplified to

$$\begin{aligned}
\int\int_S \Lambda_\mu(v,v)=&\int_{\overline{AB}\cup\overline{BC}\cup\overline{CD}}(v_{nn}v_n-v_{nnn}v)\\
&+2(1-\mu)[v_{xy}v]_C^B.
\end{aligned}\tag{5.2}$$

Moreover, the boundary norm (3.22) is expressed as

$$\begin{aligned}
\|\epsilon\|_B=&\|u-v\|_B=\sqrt{I(v)}=\{\|v-1\|_{0,\overline{AB}}^2+w_1^2\|v_n\|_{0,\overline{AB}}^2\\
&+w_1^2\|v_n\|_{0,\overline{BC}}^2+w_3^2\|v_{nnn}\|_{0,\overline{BC}}^2+w_1^2\|v_n\|_{0,\overline{CD}}^2\\
&+w_3^2\|v_{nnn}\|_{0,\overline{CD}}^2\}^{1/2},
\end{aligned}\tag{5.3}$$

where $w_i=1/(N+1)^i$. Then we have the following theorem.

Theorem 5.1. *Let $v=u_N$ in Eq. (3.17) be chosen for Model I. Suppose that the inverse inequalities hold*:

$$\begin{aligned}
&\|\epsilon_{nnn}\|_{0,\overline{AB}}\le K_N\|\epsilon\|_{2,S},\\
&\|\epsilon_{nn}\|_{0,\overline{AB}\cup\overline{BC}\cup\overline{CD}}\le K_N^*\|\epsilon\|_{2,S},
\end{aligned}\tag{5.4}$$

$$|v_{xy}(B)|\le K_N^{**}\|v_n\|_{0,\overline{BC}},\qquad |v_{xy}(C)|\le K_N^{**}\|v_n\|_{0,\overline{BC}},\tag{5.5}$$

where K_N, K_N^* and K_N^{**} may be unbounded as $N\to\infty$. Then there exist the error bounds,

$$\begin{aligned}
\|\epsilon\|_{2,S}&=\|u-v\|_{2,S}\\
&\le C(K_N+(K_N^{**}+K_N^*)/w_1+1/w_3)\|u-v\|_B,
\end{aligned}\tag{5.6}$$

where C is a bounded constant independent of N.

Proof. For $\mu\in[0,1)$ and the clamped boundary conditions on $\overline{OD}\cup\overline{AB}$, from Marti [25] and Eq. (5.2) we have

$$\begin{aligned}
\|\epsilon\|_{2,S}^2\le C|\epsilon|_{2,S}^2\le C\int\int_S\Lambda_\mu(\epsilon,\epsilon)\\
\le C\{&\|\epsilon_{nn}\|_{0,\overline{AB}}\|v_n\|_{0,\overline{AB}}+\|\epsilon_{nnn}\|_{0,\overline{AB}}\|v-1\|_{0,\overline{AB}}\\
&+\|\epsilon_{nn}\|_{0,\overline{BC}}\|v_n\|_{0,\overline{BC}}+\|v_{nnn}\|_{0,\overline{BC}}\|\epsilon\|_{0,\overline{BC}}\\
&+\|\epsilon_{nn}\|_{0,\overline{CD}}\|v_n\|_{0,\overline{CD}}+\|v_{nnn}\|_{0,\overline{CD}}\|\epsilon\|_{0,\overline{CD}}\\
&+|v_{xy}(B)||\epsilon(B)|+|v_{xy}(C)||\epsilon(C)|\}.
\end{aligned}\tag{5.7}$$

From the Sobolev embedded theorem [31], there exist the bounds,

$$\begin{aligned}
&\|\epsilon\|_{0,\overline{BC}\cup\overline{CD}}\le C\|\epsilon\|_{2,S},\qquad |\epsilon(B)|\le C\|\epsilon\|_{2,S},\\
&|\epsilon(C)|\le C\|\epsilon\|_{2,S}.
\end{aligned}\tag{5.8}$$

Hence from Eqs. (5.4), (5.7) and (5.8) we have

$$\begin{aligned}
\|\epsilon\|_{2,S}^2\le C\{&K_N^*\|v_n\|_{0,\overline{AB}}+K_N\|v-1\|_{0,\overline{AB}}+K_N^*\|v_n\|_{0,\overline{BC}}\\
&+\|v_{nnn}\|_{0,\overline{BC}}+K_N^*\|v_n\|_{0,\overline{CD}}+\|v_{nnn}\|_{0,\overline{CD}}\\
&+|v_{xy}(B)|+|v_{xy}(C)|\}\|\epsilon\|_{2,S}.
\end{aligned}\tag{5.9}$$

Moreover, from Eq. (5.5)

$$|v_{xy}(B)|+|v_{xy}(C)|\le 2K_N^{**}\|v_n\|_{0,\overline{BC}}\le 2\frac{K_N^{**}}{w_1}\|\epsilon\|_B.\tag{5.10}$$

Combining Eqs. (5.9) and (5.10) leads to

$$\begin{aligned}
\|\epsilon\|_{2,S}\le C\{&K_N^*\|v_n\|_{0,\overline{AB}}+K_N\|v-1\|_{0,\overline{AB}}+K_N^*\|v_n\|_{0,\overline{BC}}\\
&+\|v_{nnn}\|_{0,\overline{BC}}+K_N^*\|v_n\|_{0,\overline{CD}}+\|v_{nnn}\|_{0,\overline{CD}}\}\\
&+2K_N^{**}/w_1\|\epsilon\|_B\\
\le C\{&K_N+(K_N^*+K_N^{**})/w_1+1/w_3\}\|\epsilon\|_B,
\end{aligned}\tag{5.11}$$

Table 1
The computed results from Model I: the clamped condition on $\overline{AB}$ and the symmetric condition on $\overline{BC}$

N	M	E_2	Cond.	d_1	c_1
5	5	0.684(−2)	122	1.558314068	0.5439790(−1)
10	10	0.310(−3)	0.525(4)	1.579179739	0.8584309(−1)
15	15	0.172(−4)	0.897(5)	1.579103462	0.8433073(−1)
20	20	0.211(−5)	0.965(6)	1.579146775	0.8451656(−1)
25	25	0.628(−6)	0.766(7)	1.579146331	0.8455956(−1)
30	30	0.292(−6)	0.142(9)	1.579144492	0.8455695(−1)
35	35	0.141(−6)	–	1.579144356	0.8455997(−1)

where we have used Eq. (5.3). This completes the proof of Theorem 5.1. □

Note that although the corner condition $v_{xy}(B) = v_{xy}(C)$ is not imposed explicitly on v, it is also satisfied approximately based on Theorem 5.1. The analysis for the collocation Trefftz method with interior boundary conditions can be made similarly by following Ref. [20] and this paper. In fact, the assumption (5.5) can be obtained by

$$|v_{xy}(B)| \le |v_{xy}|_{\infty,\overline{BC}} \le K_1\|v_n\|_{3/2,\overline{BC}} \le K_1K_2\|v_n\|_{0,\overline{BC}} \le K_N^{**}\|v_n\|_{0,\overline{BC}}, \tag{5.12}$$

Table 2
The computed coefficients from Model I at $N = M = 30$

k	d_k	c_k
1	0.157914449154(1)	0.845569495127(−1)
2	−0.101875081011(1)	0.218682879130
3	−0.388345996362	0.147059328607
4	−0.126596391437	0.258957626846(−1)
5	−0.901531703063(−2)	−0.661047276514(−2)
6	−0.410342771786(−2)	0.692602886653(−2)
7	−0.152219180639(−1)	0.109004031831(−1)
8	−0.105644615332(−1)	0.533572185075(−2)
9	−0.353330627848(−2)	0.128477201276(−2)
10	−0.108364832609(−2)	0.799088937995(−3)
11	−0.932961247848(−3)	0.638532919383(−3)
12	−0.560626543201(−3)	0.321076862256(−3)
13	−0.217242844519(−3)	0.977392253721(−4)
14	−0.883260517136(−4)	0.702432472164(−4)
15	−0.620368652529(−4)	0.324466328939(−4)
16	−0.285719771197(−4)	0.252039158155(−4)
17	−0.232213823882(−4)	0.131914570651(−4)
18	−0.102940821331(−4)	0.666829468399(−5)
19	−0.157042167188(−5)	−0.394496927639(−5)
20	0.320173251469(−5)	0.183197951331(−5)
21	−0.572645396667(−5)	0.504462110589(−5)
22	−0.311064327607(−5)	0.563661160729(−6)
23	0.131511891651(−5)	−0.201658325294(−5)
24	0.120638425971(−5)	0.462845013470(−6)
25	−0.155256612338(−5)	0.131479847331(−5)
26	−0.667684153216(−6)	0.383815032080(−7)
27	0.230910782803(−6)	−0.222247821436(−6)
28	0.866642073153(−7)	0.784944120044(−7)
29	−0.163894984647(−6)	0.125626303448(−6)
30	−0.631610177158(−7)	0.148114879917(−7)

Table 3
The computed results from Model II: the simply supported condition on $\overline{AB}$ and the symmetric condition on $\overline{BC}$

N	M	E_2	Cond.	d_1	c_1
5	5	0.333(−2)	228	0.850292568	−0.1238970
10	10	0.568(−4)	0.678(4)	0.843682925	−0.1339992
15	15	0.280(−5)	0.106(6)	0.843237554	−0.1344272
20	20	0.138(−6)	0.111(7)	0.843266263	−0.1344504
25	25	0.330(−8)	0.961(7)	0.843265749	−0.1344259
30	30	0.234(−9)	0.672(8)	0.843265738	−0.1344254
35	35	0.151(−10)	–	0.843265743	−0.1344254

where $K_N^{**} = K_1K_2$. When S is a sector, we can show that $K_N = O(N^2)$, $K_N^* = O(N)$ and $K_N^{**} = O(N^{3/2})$.

6. Numerical experiments

We carry out the collocation Trefftz method in double precision for these crack models. For Model I, the computed results of errors, condition numbers and coefficients are given in Tables 1 and 2 with the numerical asymptotic

Table 4
The computed coefficients from Model II at $N = M = 30$

k	d_k	c_k
1	0.843265737636	−0.134425410478
2	−0.810315226397(−1)	0.555684857969(−2)
3	−0.760189138549(−1)	0.389434470960(−1)
4	−0.406409839309(−1)	0.147075362850(−1)
5	−0.107965037008(−2)	−0.873849200785(−2)
6	0.926519150105(−2)	−0.352886098194(−2)
7	−0.537688211088(−3)	0.152504271457(−2)
8	−0.159558209100(−2)	0.619084537209(−3)
9	−0.602403160151(−4)	−0.295608460532(−3)
10	0.312644128283(−3)	−0.136655913609(−3)
11	−0.171094471457(−4)	0.703637646769(−4)
12	−0.746810945381(−4)	0.332124185817(−4)
13	−0.202261881438(−5)	−0.166584246932(−4)
14	0.172358111626(−4)	−0.770462588631(−5)
15	−0.680975685900(−6)	0.381985848508(−5)
16	−0.393029468513(−5)	0.177201776927(−5)
17	−0.753002175322(−7)	−0.889681257230(−6)
18	0.908970763257(−6)	−0.413094733348(−6)
19	−0.347771312608(−7)	0.210684813352(−6)
20	−0.212002381035(−6)	0.955540479240(−7)
21	−0.117653124582(−8)	−0.496876236952(−7)
22	0.489076758087(−7)	−0.212558167696(−7)
23	−0.310394116929(−8)	0.117984903867(−7)
24	−0.106176086258(−7)	0.417122852930(−8)
25	0.436460058617(−9)	−0.242925552763(−8)
26	0.209830897613(−8)	−0.795430112067(−9)
27	−0.244865068337(−9)	0.514646524550(−9)
28	−0.366636428060(−9)	0.883960453604(−10)
29	0.436452408457(−10)	−0.557222929732(−10)
30	0.268911356390(−10)	−0.756987886739(−11)

Table 5
The computed results for the clamped condition on $\overline{AB}$ and the simply supported condition on $\overline{BC}$

N	M	E_2	Cond.	d_1	c_1
5	5	0.225(−1)	78.2	0.155100168	0.5763955
10	10	0.390(−3)	0.123(4)	0.158398736	0.5921653
15	15	0.120(−4)	0.155(5)	0.158417284	0.5921496
20	20	0.601(−6)	0.159(6)	0.158417050	0.5921666
25	25	0.435(−7)	0.153(7)	0.158417062	0.5921658
30	30	0.256(−8)	0.146(8)	0.158417061	0.5921659
35	35	0.121(−9)	–	0.158417061	0.5921659

Table 6
The computed results for the simply supported condition on $\overline{AB}$ and $\overline{BC}$

N	M	E_2	Cond.	d_1	c_1
5	5	0.549(−2)	97.1	0.106751524	0.5789919
10	10	0.136(−3)	0.146(4)	0.107175441	0.5821202
15	15	0.274(−5)	0.150(5)	0.107184297	0.5820906
20	20	0.159(−6)	0.146(6)	0.107184194	0.5820990
25	25	0.881(−8)	0.154(7)	0.107184186	0.5820988
30	30	0.535(−9)	0.146(8)	0.107184187	0.5820988
35	35	0.118(−10)	–	0.107184187	0.5820988

relations,

$$E_2 = O(0.83^N), \qquad \text{Cond.} = O(1.6^N), \tag{6.1}$$

where E_2 and Cond. are defined in Eqs. (3.22) and (3.23), respectively. For Model II, the results are listed in Tables 3 and 4, with

$$E_2 = O(0.58^N), \qquad \text{Cond.} = O(1.5^N). \tag{6.2}$$

Obviously, Model II is better than Model I as a crack model due to higher accuracy and better stability. The important leading coefficient d_1 has eight significant digits for $N = M = 30$ in Tables 2 and 4.

Note that for Models I and II, the particular solutions have $v_{xy}(B) \neq 0$ and $v_{xy}(C) \neq 0$. We may also add the corner contribution, $2(1-\mu)w_2^2\{v_{xy}^2(B) + v_{xy}^2(C)\}$, to the energy (4.13), and carry out the corresponding collocation Trefftz method. The numerical solutions obtained are only slightly different from those in Tables 2 and 4. This fact verifies well the analysis in Section 5.

Let us change the boundary conditions on $\overline{AB}$ and $\overline{BC}$ only, and retain other boundary conditions to be the same as those in Models I and II. First, choose the simply supported conditions on $\overline{AB}$ instead

$$u|_{\overline{AB}} = 1, \qquad u_{nn}|_{\overline{AB}} = 0. \tag{6.3}$$

The computed results are listed in Tables 5 and 6. Second, choose the natural conditions on $\overline{BC}$,

$$(u_{yy} + \mu u_{xx})|_{\overline{BC}} = 0, \qquad (u_{yyy} + (2-\mu)u_{xxy})|_{\overline{BC}} = 0. \tag{6.4}$$

Tables 7 and 8 list the computed results for Eq. (6.4) with $\mu = 0$ and 1/2.

From Tables 1, 3, and 5–8, we discover the following interesting facts.

(1) The clamped boundary condition will enhance the crack singularity ($K = \sqrt{2\pi}d_1$), where the leading coefficient $d_1 = 1.5791$ in Table 1 is largest.
(2) The simply supported boundary will decline the crack singularity due to release of internal force, where $d_1 = 0.10718$ in Table 6 is smallest.

Table 7
The computed results for the clamped condition on $\overline{AB}$ and the natural condition on $\overline{BC}$

N	M	$\mu = 0$				$\mu = 0.5$			
		E_2	Cond.	d_1	c_1	E_2	Cond.	d_1	c_1
5	5	0.129(−1)	96.7	1.5430987	0.0574098	0.169(−1)	101	1.5353281	0.0297869
10	10	0.541(−3)	0.438(4)	1.5539560	0.0769581	0.205(−2)	0.488(4)	1.5611910	0.0107761
15	15	0.221(−3)	0.841(5)	1.5528777	0.0711955	0.809(−3)	0.897(5)	1.5694103	0.0175093
20	20	0.775(−4)	0.900(6)	1.5544130	0.0809604	0.304(−3)	0.894(6)	1.5748700	0.0199416
25	25	0.351(−4)	0.666(7)	1.5550780	0.0865020	0.135(−3)	0.639(7)	1.5746413	0.0194029
30	30	0.175(−4)	0.698(8)	1.5555684	0.0907366	0.690(−4)	0.723(8)	1.5737998	0.0186469

Table 8
The computed results for the simply supported condition on $\overline{AB}$ and the natural condition on $\overline{BC}$

N	M	$\mu = 0$				$\mu = 0.5$			
		E_2	Cond.	d_1	c_1	E_2	Cond.	d_1	c_1
5	5	0.355(−2)	151	0.8510274	−0.1059579	0.257(−2)	165	0.8567461	−0.1418792
10	10	0.105(−3)	0.616(4)	0.8368815	−0.1252351	0.972(−4)	0.686(4)	0.8413529	−0.1629535
15	15	0.228(−4)	0.106(6)	0.8370426	−0.1249991	0.217(−4)	0.117(6)	0.8412125	−0.1634846
20	20	0.545(−5)	0.105(7)	0.8369060	−0.1251114	0.452(−5)	0.114(7)	0.8409659	−0.1639608
25	25	0.192(−5)	0.773(7)	0.8368681	−0.1251136	0.139(−5)	0.825(7)	0.8408906	−0.1641277
30	30	0.113(−5)	0.847(8)	0.8368767	−0.1250077	0.623(−6)	0.929(8)	0.8408885	−0.1640853

Table 9
The computed results from the model of Schiff et al. [30] with $a = 0.4$ and $b = 0.7$

N	M_1	M_2	E_2	Cond.	d_1	c_1
7	7	6	0.202(−2)	0.729(3)	−0.12545711	−0.84205789
14	14	16	0.161(−3)	0.724(5)	−0.12650102	−0.94471478
21	21	24	0.237(−4)	0.557(7)	−0.12650639	−0.94411067
28	28	32	0.585(−5)	0.357(9)	−0.12650611	−0.94427916

Table 10
Comparison on some nodal solutions from the model of Schiff et al. [30] with $a = 0.4$ and $b = 0.7$

x	y	Refinement [30]	Whiteman [33]	Collocation Trefftz method
−0.1	0.1	20.2	20.2	20.15
0	0.1	146.5	146.6	146.54
0.1	0.1	617.3	617.3	617.28
0.1	0	508.1	508.1	508.11
−0.2	0.2	23.8	23.8	23.82
0	0.3	503.5	503.7	503.59
0.2	0.2	1515.5	1515.5	1515.58
0.3	0.1	2321.8	2321.6	2321.83
−0.2	0.4	123.4	123.4	123.46
0	0.5	722.5	722.8	722.50
0.2	0.4	1703.2	1703.2	1703.21

(3) The symmetric boundary condition results from symmetry of the solution. The effects of the natural conditions on d_1 are slightly less than those of the symmetric condition by comparing Tables 7 and 8 with Tables 1 and 3.

All these conclusions agree with our physical intuition. We also expect coefficient d_1 would be larger from Model III than that from Model I, where the clamped boundary condition is subjected on the entire boundary ∂S. The computed coefficient $d_1 = 2.1275$ given in Table 14 later confirms such an expectation.

Table 11
Comparison of leading coefficients for the model of Schiff et al. [30] with $a = 0.4$ and $b = 0.7$

d_i and c_i	Refinement [30]	Whiteman [33]	Collocation Trefftz method
d_1	1.2649	1.2651	1.2650611
d_2	−0.9354	−0.9361	−0.9360218
d_3	−0.8013	−0.7985	−0.8010796
d_4	−1.0040	−0.9961	−0.9976181
c_1	−0.0945	−0.0944	−0.0944279
c_2	0.1007	0.1004	0.1011681
c_3	0.4684	0.4603	0.4641121

Table 12
The computed coefficients from the model of Schiff et al. [30] with $a = 0.4$ and $b = 0.7$

k	d_k	c_k
1	0.126506110061(1)	−0.944279161457(−1)
2	−0.936021839307	0.101168072395
3	−0.801079627221	0.464112132938
4	−0.997618091594	0.396464688101
5	−0.105301853401(1)	0.123461423186(1)
6	−0.229836599320(1)	0.120497827195(1)
7	−0.124156774129(1)	0.155145289337(1)
8	−0.381641467043(1)	0.310537969427(1)
9	−0.238720411821(1)	0.173097719915(1)
10	−0.591294036802(1)	0.733160209882(1)
11	−0.555017829366(1)	0.572735184513
12	−0.638776268248(1)	0.151705915581(2)
13	−0.151886092148(2)	−0.501804399258
14	−0.245308286590(1)	0.263242128941(2)
15	−0.369114292099(2)	0.232732717009(1)
16	0.105446614959(2)	0.351213245198(2)
17	−0.758820662861(2)	0.223936816349(2)
18	0.268975706382(2)	0.324998364448(2)
19	−0.125018972003(3)	0.735139264579(2)
20	0.245844631003(2)	0.166808451244(2)
21	−0.157558912596(3)	0.143594590248(3)
22	−0.156534339595(2)	0.268733725020(1)
23	−0.145629281481(3)	0.184742907459(3)
24	−0.750616959430(2)	0.742968495770(1)
25	−0.904763921775(2)	0.149922923157(3)
26	−0.938412699634(2)	0.194247065221(2)
27	−0.303834486338(2)	0.646114763546(2)
28	−0.535812083701(2)	0.174429927114(2)

Next, we carry out the models of Schiff et al. In computation, take parameters $a = 0.4$ and $b = 0.7$ as in Ref. [30], and choose the uniform partition on ∂S. Denote by M_1 and M_2 the partitions number of $\overline{AB}$ and $\overline{BC}$. Tables 9–12 list the computed results. It can be seen that the computed results coincide very well with other methods given in Refs. [30,33].

When parameters $a = b = 1$, the model of Schiff et al. is our Model III with the clamped conditions in Eqs. (3.9)–(3.13). The computed results are provided in Tables 13 and 14. It can be seen that the solutions have slower convergence than those of Models I and II. Interestingly, the leading coefficient of d_1 in Model III for $N = M = 30$ also has seven significant digits, see Table 13.

Table 13
The computed results from Model III of Schiff et al. [30] with $a = b = 1$

N	M	E_2	Cond.	d_1	c_1
5	5	0.382(−1)	75.3	2.0562025	0.12853961
10	10	0.112(−2)	0.908(3)	2.1270176	0.16689967
15	15	0.205(−3)	0.864(4)	2.1275137	0.16675604
20	20	0.510(−4)	0.756(5)	2.1275130	0.16676800
25	25	0.142(−4)	0.675(6)	2.1275131	0.16676291
30	30	0.622(−5)	–	2.1275135	0.16676210

Table 14
The computed coefficients for Model III of Schiff et al. [30] with $a = b = 1$ at $N = 30$ and $M = 30$

k	d_k	c_k
1	0.212751351189(1)	0.166762096608
2	−0.103669248813(1)	0.624433242670(−1)
3	0.371710686206(−1)	−0.132473844421
4	0.117748896104	−0.102209420793(−1)
5	−0.122728218338	0.105845606844
6	−0.109908664317	0.311525254876(−1)
7	−0.225523569851(−2)	−0.714919699164(−2)
8	0.686312696358(−2)	−0.168432409440(−2)
9	−0.593565985657(−2)	0.948384227186(−2)
10	−0.110320364140(−1)	0.428077318143(−2)
11	−0.372990401057(−3)	−0.251437034002(−3)
12	−0.434606261276(−3)	0.300065928400(−3)
13	0.395471328942(−3)	−0.279833704674(−3)
14	−0.363701441420(−3)	0.415900781575(−3)
15	0.849752152135(−4)	−0.394160763591(−3)
16	0.164814091626(−3)	0.137207394892(−3)
17	−0.134885562580(−3)	0.114185322520(−4)
18	−0.661256038945(−4)	0.128433796144(−3)
19	−0.442704344901(−4)	−0.895164048915(−4)
20	0.881231488859(−4)	0.101254396117(−4)
21	−0.513612091552(−4)	0.237215483998(−4)
22	−0.185089281333(−4)	0.287229819371(−4)
23	−0.110577269133(−4)	−0.290039116621(−4)
24	0.383799694523(−4)	−0.783857638552(−5)
25	−0.193733376681(−4)	0.200879527653(−4)
26	−0.123722918845(−4)	0.597917917868(−5)
27	−0.218094975397(−5)	−0.273563392080(−5)
28	0.496907945145(−5)	−0.185227194727(−5)
29	−0.211257805760(−5)	0.303478369806(−5)
30	−0.189383438010(−5)	0.462805951252(−6)

In summary, in this section we have provided the numerical solutions for Models I–III by the collocation Trefftz method. The advantage of Model II (as well as Model I) over Model III is that only one crack singularity exists at the origin. Note that in Model III, there may exist a mild singularity at the corners B and C from the clamped boundary condition, see Lefeber [18], p. 55. We carry out the collocation Trefftz method by Mathematica using the working decimal digits

Table 15
Comparisons on E_2 from Models II and III, where Pre. is the working precision digits used in Mathematica

N	Pre.	E_2 (Model II)	ln E_2	E_2 (Model III)	ln E_2
5	20	0.149(−2)	−2.83	0.382(−1)	−1.42
10	20	0.929(−5)	−5.03	0.112(−2)	−2.95
20	30	0.207(−7)	−7.68	0.510(−4)	−4.29
30	40	0.351(−10)	−10.56	0.622(−5)	−5.21
40	50	0.104(−12)	−12.98	0.205(−5)	−5.69
50	60	0.216(−15)	−15.66	0.629(−6)	−6.20
60	70	0.820(−18)	−18.09	0.291(−6)	−6.54
70	80	0.152(−20)	−20.82	0.167(−6)	−6.78
80	90	0.710(−23)	−23.15	0.101(−6)	−7.00
90	100	0.119(−25)	−25.92	0.633(−7)	−7.20
100	100	0.648(−28)	−28.19	0.424(−7)	−7.37

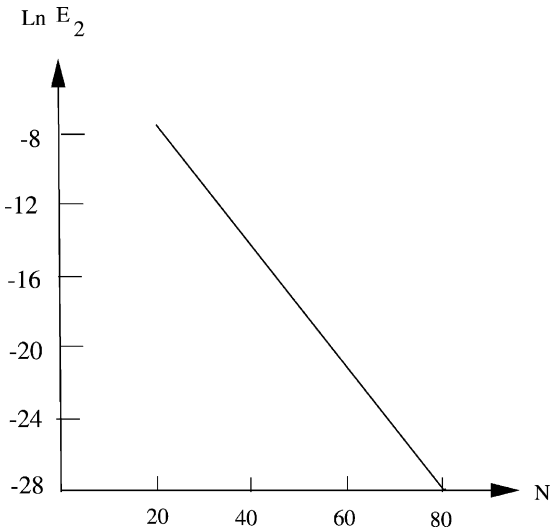

Fig. 9. The error curves of E_2 from Model II.

Pre. ≤ 100, and the errors are listed in Table 15 for Models II and III. The error curves given in Figs. 9 and 10 display that Model II yields exponential convergent rates, but Model III does not. This fact indicates existence of a corner singularity in Model III. Since Model III provides much larger errors shown in Table 15, Models II and III are better crack models and Model II is the best crack model of singularity problems for biharmonic equations. To give a clear view, profiles of the solutions from Model II are provided in Fig. 11.

It is worth pointing out that the approximate solutions of three models converge slower than those of the Motz's problem in Ref. [20]. This result is reasonable because the biharmonic equations are more complicated than Laplace's equation.

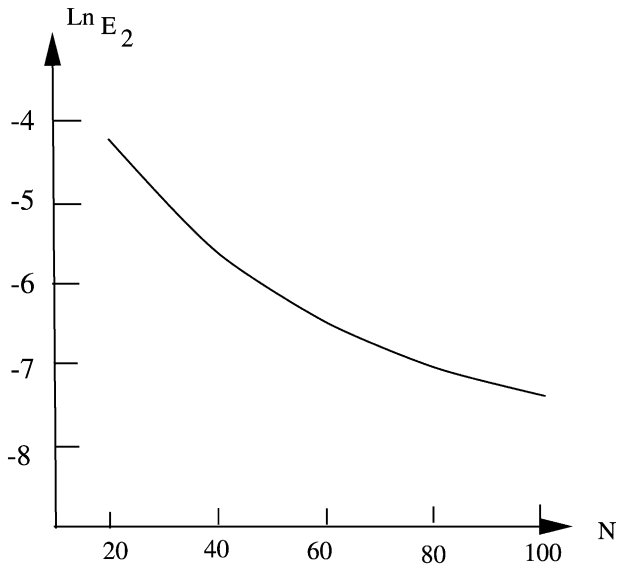

Fig. 10. The error curves of E_2 from Model III.

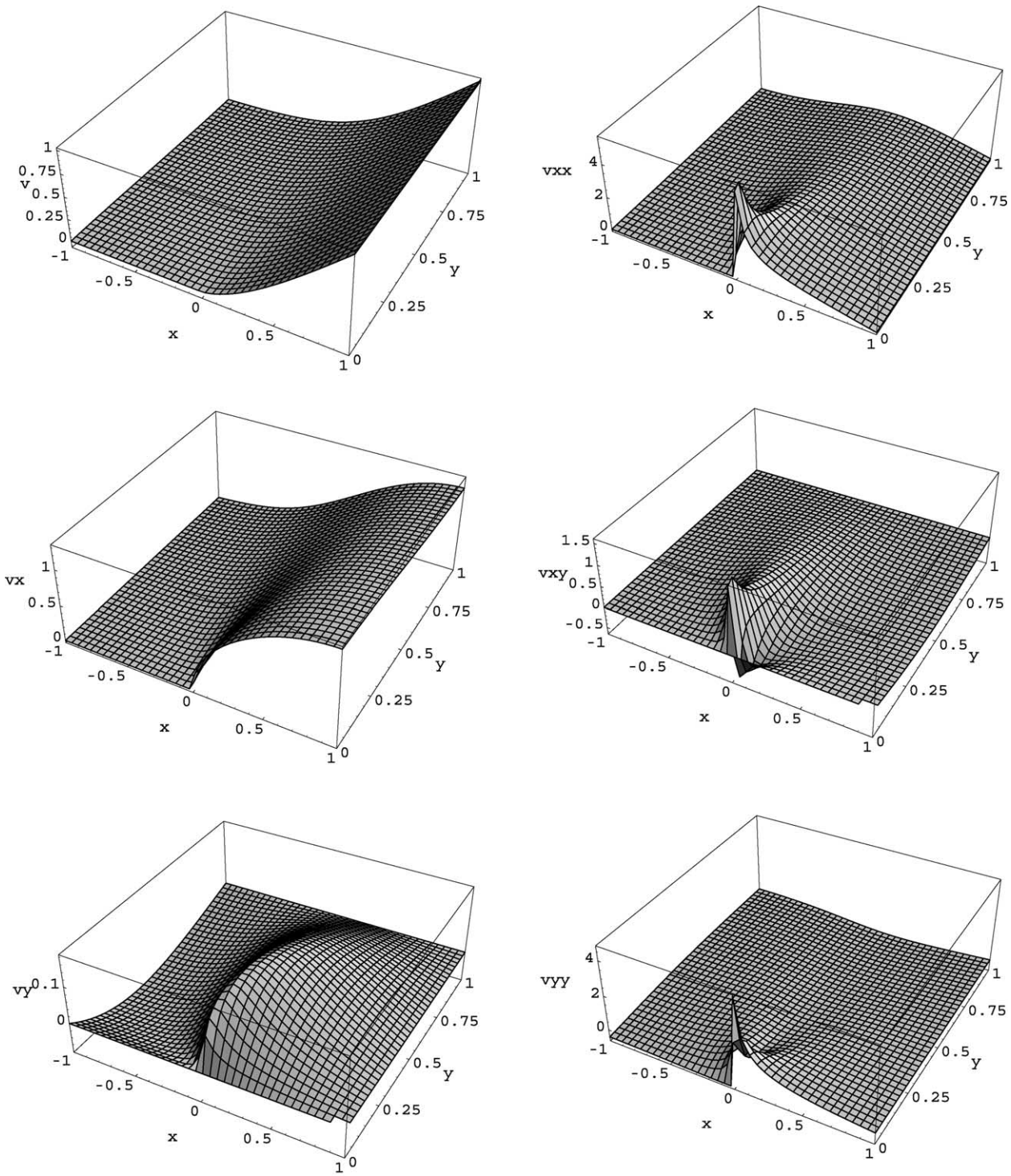

Fig. 11. Profiles of the solutions from Model II.

7. Concluding remarks

To conclude this paper, let us address a few remarks.

1. The terms, $(u_{ns}^{+} - u_{ns}^{-})v$ at the corners and $u_{ns}v$ at those with the right angles, are developed for the Green formulas of biharmonic equations on polygons. The corner terms coincide with those in Chien [5], also see Remark 2.1. Those terms are important to the natural corners, to yield the corner condition $u_{ns}^{+} = u_{ns}^{-}$, which indicates in physics that the corner angles of thin plates keep invariant. Also based on the Green formulas, the interior continuity conditions, $u^{+} = u^{-}$, $u_{n}^{+} = u_{n}^{-}$, $u_{nn}^{+} = u_{nn}^{-}$ and $u_{nnn}^{+} = u_{nnn}^{-}$ on Γ_0, are derived.
2. Error bounds in Section 5 are derived for a brief analysis, which provides a justification for the collocation Trefftz

method, and the computational formulas of partial derivatives of the series solutions in Section 3.4 are provided for the collocation Trefftz method in computation.

3. Two new crack models I and II are proposed, which resemble Motz's problem in Ref. [20] with only one crack singularity. Also Model III results from Schiff et al. [30].
4. The collocation Trefftz method (i.e. the BAM in Refs. [20,23]) are proposed to provide the most accurate solutions in double precision for three models. The exponential convergence rates are obtained for Models I and II, but not for Model III. The slow convergence of Model III shown in Table 15 displays existence of mild corner singularities in the model, which is explored in Ref. [12] in detail.
5. Model II with higher convergent rates is recommended for crack models, whose leading coefficient d_1 is obtained with eight significant decimal digits. The crack models are important to test numerical methods, and the very accurate solutions given in this paper may be used as the true solutions, to evaluate errors of other numerical methods, see Ref. [23].
6. This paper is an important extension of the collocation Trefftz method (i.e. the BAM [20]) for crack singularity of biharmonic equations. This method may also be regarded as a variant of the boundary element method (BEM). Particular solutions are chosen instead of fundamental solutions in BEM, and only the boundary conditions need to be fitted as best as possible. The most remarkable advantage of the collocation Trefftz method (as well as BEM) is reduction from the PDE problems in the whole domain S to the problems on the boundary ∂S only, which greatly saves the CPU time and the computer storage. The drawback of the collocation Trefftz method is that the particular solutions must be *known* and *explicit*; this confines the collocation Trefftz method to some simple equations in simple solution domains. A compensation for this drawback is to invoke the combined methods described in Ref. [23], where the collocation Trefftz method may be used in the sub-domains with singularities, or in the vast regions for the CPU saving, while the FEM is chosen for the smooth subdomains.
7. Let us compare the collocation Trefftz method with BEM. For the collocation Trefftz method, the computational algorithms are much simpler, and the explicit solutions, in particular the explicit leading coefficient d_1, directly computed by the collocation Trefftz method is more attractive and useful in engineering problems. More importantly, the collocation Trefftz method may provide the *most accurate* solutions, see Ref. [23], which may be regarded as the true solution, to evaluate errors of other numerical methods.
8. The interior and exterior boundary conditions and the corner conditions in this paper can be applied to the collocation methods using the radial basis functions or the Sinc functions, etc. because the collocation Trefftz method can be viewed as a special kind of boundary collocation methods using the particular solutions of the equations. A further study of general collocation methods for biharmonic equation appears elsewhere.
9. The solution domains of numerical experiments in this paper are assumed to be a rectangle, and the accuracy of the numerical solutions is very high. In fact, the numerical approaches of collocation Trefftz methods in this paper can be easily applied to a polygonal domain, and even to a closed domain, see ">Remark 2.1. However, when the object domain is narrow and complicated, the computational accuracy may be worse. Some deteriorated results on narrow domain can be found in Ref. [12].

Acknowledgements

We are grateful to the reviewers for their valuable comments and suggestions, and also express our thanks to Ya-Ling Chen and Chung-Hua Hsu for some works in Section 3.4 and Table 15.

References

[1] Arad A, Yakhot A, Ben-Dor G. A highly accurate numerical solution of a biharmonic equation. Numer Meth Partial Differential Equations 1997;13:375–97.
[2] Birkhoff G, Lynch RE. Numerical solution of elliptic equations. Philadelphia: SIAM; 1984.
[3] Brebbia CA, Dominguez J. Boundary elements, an introduction course. New York: SIAM-Hill Book Company; 1989.
[4] Carey GF, Oden JT, Finite elements, a second course, vol. II. Englewood Cliffs, NJ: Prentice-Hall; 1983.
[5] Chien WZ. Variational and finite element methods (in Chinese). Taipei: East Asia Publishing; 1989.
[6] Courant R, Hilbert D, Methods of mathematical physics, vol. I. New York: Wiley; 1953.
[7] Gourgeon H, Herrera I. Boundary methods c-complete systems for the biharmonic equations. Boundary element methods (Irvine, CA). CML Publications, Berlin: Springer; 1981. p. 431–41.
[8] Grisvard P. Elliptic problems in non-smooth domains. Pitman advanced publishing program, Boston; 1985.
[9] Herrera I. Unified formulation of numerical methods. Part I. Green's formulas for operators in discontinuous fields. Numer Meth Partial Differential Equations 1985;1:25–44.
[10] Herrera I, Diaz M. Indirect methods of collocation: Trefftz–Herrera collocation. Numer Meth Partial Differential Equations 1999;15:709–38.
[11] Herrera I. Boundary methods: an algebraic theory. London: Pitman; 1984.
[12] Hsu CH. Biharmonic boundary value problem with singularity. Master thesis, Department of Applied Mathematics, National Sun Yat-sen University; 2002
[13] Jin WG, Cheung YK, Zienkiewicz OC. Trefftz method for Kirchoff plate bending problems. Int J Numer Meth Engng 1993;36:765–81.

[14] Jirousek J, Guex L. The hybrid-Trefftz finite element model and its application to plate bending. Int J Numer Meth Engng 1986;23: 651–93.
[15] Karageorghis A. Modified methods of fundamental solutions for harmonic and biharmonic problems with boundary singularities. Numer Meth Partial Differential Equations 1992;8:1–18.
[16] Kita E, Kamiya N. Trefftz method, an overview. Adv Engng Software 1995;24(1–3):3–12.
[17] Kolodziej J. Review of application of boundary collocation methods in mechanics of continuous media. SM Arch 1987;12(4):187–231.
[18] Lefeber D. Solving problems with singularities using boundary elements. Southampton: Computational Mechanics Publications; 1989.
[19] Leitao V. Application of multi-region Trefftz-collocation to fracture mechanics. Engng Anal Bound Elem 1998;22:251–6.
[20] Li ZC, Mathon R, Serman P. Boundary methods for solving elliptic problem with singularities and interfaces. SIAM J Numer Anal 1987; 24:487–98.
[21] Li ZC, Mathon R. Boundary methods for elliptic problems on unbounded domains. J Comput Phys 1990;89:414–31.
[22] Li ZC, Mathon R. Error and stability analysis of boundary methods for elliptic problems with interfaces. Math Comput 1990;54:41–61.
[23] Li ZC. Combined methods for elliptic equations with singularities, interfaces and infinities. Boston: Kluwer; 1998.
[24] Lucas TR, Oh HS. The method of auxiliary mapping for the finite element solutions of elliptic problems containing singularities. J Comput Phys 1993;108:327–42.
[25] Marti JT. Introduction to Sobolev spaces and finite element solutions of elliptic boundary value problems. London: Academic Press; 1986.
[26] Motz M. The treatment of singularities of partial differential equations by relaxation methods. Quart Appl Math 1947;4:371–7.
[27] Piltner R, Taylor RL. The solution of plate blending problems with the aid of a boundary element algorithm based on singular complex function. Boundary elements XII. Proceedings of the 12th World Conference on BEM, Sapporo, Japan; 1990. p. 437–45.
[28] Roos HG, Stynes M, Tobiska L. Numerical methods for singularly perturbed differential equations, convection–diffusion and flow problems. Berlin: Springer; 1991.
[29] Russo R. A Green formulas for plane crack problems. Boll Un Mat Ttal 1987;A(7)(1):59–67.
[30] Schiff BD, Fishelov D, Whitman JR. Determination of a stress intensity factor using local mesh refinement. In: Whiteman JR, editor. The mathematics of finite elements and applications III. London: Academic Press; 1979. p. 55–64.
[31] Sobolev SL. Application of functional analysis in mathematical physics. Providence, RI: AMS; 1963.
[32] Trefftz E. Ein Gegenstuck zum Ritz'schen Verfahren. Proc Second Ind Cong Appl Mech, Zurch 1926;131–7.
[33] Whitman JR. Numerical treatment of a problem from linear fracture mechanics. In: Owen DRJ, Luxmoore AR, editors. Numerical methods in fracture mechanics. Swansea: University of Wales; 1978. p. 128–36.